High-resolution spatiotemporal analysis of hydrologic connectivity in the historical floodplain of straightened lowland agricultural streams

Marchand, Jean-Philippe (J.-P.)[a]*, Biron, Pascale (P.M.)[a], Buffin-Bélanger, Thomas (T.)[b], Larocque, Marie (M.)[c]

[a]Department of Geography, Planning and Environment, Concordia University, Montreal, Quebec H3G 1M8, Canada

Département de biologie, chimie et géographie, Université du Québec à Rimouski, Rimouski, Quebec, G5L 3A1, Canada

[c]Département des sciences de la Terre et de l'atmosphère , Université du Québec à Montréal, Montreal, Quebec, H3C 3P8, Canada

* Corresponding author: jean-philippe.marchand@mail.concordia.ca

Other authors address:

Pascale Biron: pascale.biron@concordia.ca

Thomas Buffin-Bélanger: thomas_buffin-belanger@uqar.ca

Marie Larocque : larocque.marie@uqam.ca

ACKNOWLEDGEMENTS

Funding by the Natural Sciences and Engineering Research Council of Canada (NSERC) and by Environment and Climate Change Canada through scholarship and research funds is gratefully acknowledged. We would also like to thank William Massey, Audrey-Anne Loiselle, Max Hurson, Laurence Brunelle, Sylvain Gagné, Simon Tremblay, and Maryse Doucet for their help with fieldwork and laboratory analyses. We also give huge thanks to the agricultural producers who granted access to their land, especially the

Parentall Farm (St-Robert, QC) with whom we look forward to implement a restoration project of artificially abandoned meanders.

ABSTRACT

In agricultural watersheds, human interventions such as channel straightening have disrupted the hydrologic connectivity between headwater streams and their riparian environment and have thus undermined the ecological services provided by these small streams. Knowledge of the hydrologic connectivity between these streams and their immediate environment (shallow riparian groundwater in the historical floodplain and on adjacent hillslopes) in human-impacted settings is critical for understanding and restoring these hydrological systems but remains largely incomplete. The objective of this research is to investigate the hydrogeomorphological conditions controlling hydrologic connectivity in the historical floodplain of straightened lowland streams. Detailed measurements on the spatiotemporal variability of groundwater-surface water interactions between straightened reaches, historical floodplain including abandoned meanders, and the adjacent hillslopes were obtained using a dense network of piezometers at two sites in the St. Lawrence Lowlands (Quebec, Canada). Results show that the complex mechanisms controlling hydrologic connectivity in naturally meandering lowland rivers also operate in highly disturbed straightened reaches, despite backfilling and agricultural practices. The pre-straightening hydrogeomorphological configuration of the floodplain partly explains the complex patterns of piezometric fluctuations observed at the sites. The apex of the abandoned meanders stands out as a focal area of hydrologic connectivity as water levels indicate pressure transfer that may reflect flows from the stream, the hillslopes, and the surrounding historical floodplain. These unique field observations suggest that abandoned meanders should be promoted as key elements of restoration strategies in lowland agricultural straightened headwater streams.

Keywords: channelized agricultural headwater stream; Stream restoration; Groundwater; Floodplain, Abandoned meander; Hydraulic head

1. INTRODUCTION

Historically, much investment and effort have been placed into the rapid drainage of water during the flood season and during periods of heavy rainfall to increase field productivity in agricultural watersheds of temperate regions. This led to major morphological modifications, such as the straightening and deepening of meandering streams, over the 20th century in Europe and North America, which have particularly affected small headwater streams in lowland agricultural settings (Brookes, 1987; Wohl, 2018). The wide-ranging consequences of these interventions on the fluvial system include earlier and higher flood peaks (Schumm et al., 1984; Hupp, 1992; Wyzga, 1996), longer and lower low-water levels (Schilling et al., 2004; LaSage et al., 2008), modification of the spatiotemporal patterns of sediment transport (Brookes, 1987; Simon, 1989; Rousseau & Biron, 2009; Graf et al., 2016), reduction of aquatic (Trautman & Gartman, 1974; D'Ambrosio et al., 2014; Käiro et al., 2017) and terrestrial biodiversity (Hupp, 1992; Franklin et al., 2009), and decreased vertical and lateral hydrologic connectivity (Wohl, 2018).

A growing number of approaches now promote the restoration of natural hydrogeomorphological processes rather than fluvial landforms (Kondolf et al., 2006; Beechie et al., 2010; Wohl et al., 2015). Process-based restoration aims to increase the resilience of fluvial systems to changes in the hydrological and sediment-transport regime, e.g., extreme events, which is particularly important in the context of rapid climatic changes (Buffin-Bélanger et al., 2015). Increased hydrologic connectivity between degraded streams and their historic floodplain, including their abandoned meanders, is widely recognized as a means to improve the ecological condition and resilience of rivers (Beechie et al., 2010; Gumiero et al., 2013; Phillips, 2013; Wohl et al., 2015) . In this context, hydrologic connectivity refers to the level of connection between surface waters and the groundwater reservoir of a fluvial system through water

exchange and pressure transfer. Increased hydrologic connectivity can be achieved by combining active restoration methods (e.g., remeandering, removal of levees, raising the river bed) or by promoting more passive approaches such as freedom space for rivers (e.g., delimiting a space where the river can flood and migrate freely) (Biron et al., 2014; Massé et al., 2020). Despite the many advances in conceptualizing hydrologic connectivity within fluvial systems and developing restoration approaches, straightened lowland headwater streams in agricultural settings still receive limited attention (Liu et al., 2014). Most restoration projects in small degraded lowland rivers do not include improvement of hydrologic connectivity in their design objectives (Boulton, 2007; Wohl et al., 2015) despite the known ecological benefits of promoting hyporheic exchanges in small lowland rivers (Hester & Gooseff, 2010; Kasahara & Hill, 2006; Wohl et al., 2015).

Important questions remain unanswered regarding the extent of hydrologic connectivity between straightened lowland headwater streams and their associated floodplain and hillslopes. This is particularly true in rural regions where streams have been backfilled and are often located in cultivated areas. The straightening and deepening of small lowland streams lower the water table in the near-stream zone (Pierce & King, 2017) and reduce the spatial extent of bank transient storage in the riparian zone (Schilling et al., 2006; Schilling & Jacobson, 2014). Embankments along channelized lowland streams can also reduce surface-groundwater exchanges with the floodplain (Clilverd et al., 2013). Nonetheless, few studies have focused on patterns and controls on surface-subsurface hydrological or pressure exchanges within straightened lowland streams (Pierce & King, 2017) and on the potential role of their riparian zones for restoring ecological processes (Liu et al., 2014).

The St. Lawrence Lowlands (Quebec, Canada) is a vast agricultural area that shelters at least 30 000 km of straightened streams (Rousseau & Biron, 2009). In this study, a unique data set of piezometric time series, at an unprecedented spatiotemporal resolution, combined with detailed topographic and stratigraphic survey data are used to analyze small-scale surface-groundwater interactions between straightened

headwater streams in the St. Lawrence Lowlands, their historical floodplains, including abandoned meanders, and hillslopes. We hypothesized that despite severe perturbations, the historical floodplain and hillslopes remain partially hydrologically connected to the straightened channel through subsurface interactions, as observed in unperturbed lowland meandering rivers (Cranswick & Cook, 2015; Larocque et al., 2016). The objective of this study is thus to investigate the hydrogeomorphological parameters controlling the level of hydrological connectivity in straightened lowland headwater streams, with a focus on the subsurface component, as a step toward the identification of novel process-based restoration approaches for these degraded agricultural streams.

2. METHODOLOGY

2.1 Study Sites

We selected two sites in the St. Lawrence Lowlands that are representative of straightened headwater streams in agricultural areas: Petit-Pot-au-Beurre (PB) and Martin (Ruisseau Martin, RM) streams. Both streams have nivo-pluvial hydrological regimes (high waters in early spring due to snow melt, an upsurge in autumn and low water in summer).

The Petit-Pot-au-Beurre stream is a small second-order stream having a drainage area of 12.8 km^2 (Figure 1). The watershed is mostly covered (approx. 90%) by crop fields (corn, soybean, and fodder plants). Our study site (stream elevation approximately 15 m a.s.l.) encompasses one abandoned meander, the surrounding historical floodplain, and the adjacent hillslope (Figure 1). The amplitude of the former meanders in the 1-km studied reach varies between 10 and 52 m. Bankfull width and depth are approximately 3 m and 1.5 m, respectively. The average annual discharge at the on-site gauging station is 0.2 m^3/s with an annual peak discharge slightly greater than 3 m^3/s. The stream can dry out during the summer. The channel was straightened between 1964 and 1966, and backfill material was placed upon the former channel and the floodplain, erasing most topographic features. A shallow half-circular

depression is the only remnant of surface topography from the pre-straightening floodplain. No subsurface drainage is present in the study area.

Figure 1:

The Ruisseau Martin (RM) is a midsize, second-order stream having a drainage area (26 km^2) that is 90% covered by agricultural fields of mainly maize and corn (Figure 2). The average historical meander amplitude and floodplain width average are 60 and 80 m, respectively. The modern channel bankfull width and depth are 5 m and 2 m, respectively. The average annual RM discharge is 1.5 m^3/s at the on-site gauging station. We monitored two sites along a 500 m reach of RM. The RM-UP site encompasses a 41-m wide abandoned meander having a floodplain on either side of the channel (note that all references to left and right in this paper are when looking downstream). The RM-DS covers a 22-m wide abandoned meander and the surrounding left floodplain (Figure 2). The channel was straightened between 1965 and 1966, but no backfilling was added to the floodplain. Thus, the straightened channel flows through an undisturbed floodplain that is bounded by a 3-m high hillslope on both sides. Small gullies have formed in the left-side hillslope, indicating potential surface runoff during precipitation events. The studied sites were cultivated until the 1980s. Since then, no cultivation has taken place, and natural (unassisted) colonization by vegetation has occurred. This site allows observation of a fully mature forest, including shrub and forested swamps and herbaceous marshes. This site allowed observation of the evolution of a straightened channel and floodplain following completely passive vegetation restoration (40 years). No subsurface drainage is present in the study area.

Figure 2.

2.2 Topographic and Stratigraphic Surveys

We performed high-resolution topographic and stratigraphic surveys at each of the three abandoned meanders (PB, RM-UP, RM-DS) to circumscribe the spatial extent of the alluvial material of the floodplain

and to position field sensors to record surface and subsurface water fluctuations. Surface topography was measured with a Total Station (Leica TC805L) and georeferenced with a DGPS (differential GPS, model Spectra precision 80). The vertical precision of the DGPS varied between 2 and 4 cm. We assessed the stratigraphy from several boreholes on the floodplain and adjacent hillslope. The excavation of the boreholes was conducted using either an auger (83 mm diameter, 0.50 m length) and up to three 1 m extensions or using a manual gas-powered drill (Pionjar 120) that produced samples of 51 mm (2 in) in diameter and 1 m in length, up to a maximum of 3.35 m. We based our unit differentiation on in situ visual assessments of colour, texture, and organic material in sediment samples collected at regular depths from the boreholes. We also dug larger pedons (1 m width, 1.5–1.7 m depth) at several locations to assess bedding structures within the alluvial unit.

We used the collected sediment samples from the boreholes for grain-size analyses. Coarse fractions (0.08-2 mm) were assessed with a sieve column, whereas we used a sedimentary column and pycnometer to determine the fine fractions (Poppe et al., 2000). The hydraulic conductivity of the different units was estimated from the grain-size distribution using HydrogeosieveXL software (Devlin, 2015). We also performed slug tests in all piezometers, using 25 cm and 50 cm water column injections, and estimated hydraulic conductivity using the Hvorslev (1951) method.

2.3 Surface Water Measurements and Piezometric Surveys

The stream stage elevation in the studied reaches was measured continuously at 30 min intervals using pressure transducers inserted within pipes installed in the stream bank. Hydraulic heads in the artificially abandoned channel, in the historical floodplain, and on the hillslope were monitored with pressure transducers installed in piezometers with data recorded at 30 min intervals. Piezometers were installed along lines running perpendicular and parallel to the current channel. Additional loggers were then

159 installed in relation to floodplain configuration. The former channel and floodplain configuration was
160 assessed using LiDAR data (light detection and ranging) and historical aerial photographs.

161 Piezometers were installed using a manually operated drill with 1.5" PVC pipes having a 40-cm perforated
162 section at the bottom. Maximum piezometer depth was determined by the depth of the alluvial unit,
163 which was in turn determined through visual assessment of the stratigraphy. The annular space around
164 the PVC pipes was filled with coarse sand and bentonite at the top. Different pressure transducers were
165 used (*Onset Hoboware Titanium*, *Solinst Levelogger Gold Junior* and *Edge model 3001*). At each site, a
166 *Solinst Barologger* was used for barometric compensation.

167 We excluded data from January and February (winter) to avoid ice cover effects on surface water heads.
168 The longest time series spans from October 2017 to June 2020; the shortest spans from August 2018 to
169 June 2020. We compiled hourly precipitation for these time series using data from the closest
170 Environment and Climate Change Canada weather stations (each site is less than 20 km from a station).
171 On-site hunting cameras allowed to confirm that rain events measured at the weather stations occurred
172 at the study sites.

173 We used cross-correlation analyses to assess interactions between the piezometer time series and the
174 channel stage at an event-based scale. Although cross-correlation analyses can be applied to a complete
175 time series (Larocque et al., 2016), event-based applications are more applicable to smaller spatial and
176 temporal scales (Buffin-Bélanger et al., 2016). These analyses were thus only performed during large
177 hydrological events in the channel (i.e., events that triggered a minimum stream level rise of 0.25 m). We
178 documented approximately 40 events at each site over 2.5 years. The end of a hydrological event was
179 determined either from a new rise in water levels in the channel or from water levels in the channel
180 reaching a pre-flood level. Care was taken to avoid complex hydrological events from cross-correlation
181 analyzes, including multiple consecutive increases occurring over short periods. The lag time

corresponding to the maximum cross-correlation coefficient (MCCC) between river levels and head data were estimated for all events and all piezometers. A MCCC value close to 1 with a lag time of zero indicates that both fluctuations (in the channel and in the piezometer) are almost synchronous and that their hydrographs have similar shapes. Negative time lags indicate that the fluctuation in the piezometer precedes the fluctuation in the channel. This cross-correlation analysis of channel-floodplain peak stages assumes that large MCCC and short lag times indicate a greater potential for hydrological interactions. It should be noted here that this type of analysis is based on hydraulic pressure gradients, which only infer pressure exchanges, and not directly hydrological fluxes.

At the event-based scale, we documented for each event the ratio of the amplitude of water-level fluctuations in the piezometers compared with those in the channel (hereafter Average Amplitude ratio) and the ratio of the duration of the rising limb in the piezometers compared with that in the channel (hereafter Average duration ratio). We visually interpreted the full hydraulic head time series to characterize the hydraulic gradients between the straightened streams, their respective historical floodplain, and the adjacent hillslopes in terms of magnitude and orientation at a seasonal time scale. Event-based and seasonal piezometric patterns were classified either as “flood” or “low-flow” periods to facilitate interpretation. The studied streams display two flood periods (March to mid-May and mid-October to December) and one low-flow period (mid-May to mid-October).

3. RESULTS

3.1 Stratigraphy

3.1.1 Petit-Pot-au-Beurre (PB)

At the PB site, the stratigraphic logs reveal backfilling, alluvial, and regional units (Figure 3). The backfilling unit is a deposit of poorly sorted clay with silt of a highly variable thickness (thin near the former hillslope and thicker above the historical floodplain). The alluvial unit, ranging between 0.70 and 2.00 m in

thickness, can be subdivided into four subunits arranged in complex assemblage, each representing a depositional feature, namely overbank deposits, point bars, bedload material, and floodplain topsoil. The bottom surface morphology of the alluvial unit is concave, with its deepest part near the abandoned meander apex (Figure 3). The regional unit is a sandy silt deposit, described as a shallow marine deposit from the St. Lawrence Lowland (Ministère des Ressources naturelles et de la Faune du Québec, 2012) with a gley horizon at the bottom. The average hydraulic conductivity values for the regional and the alluvial units are 1.15×10^{-7} and 1.09×10^{-5} m/s, respectively.

Figure 3.

3.1.2 Ruisseau Martin (RM)

The RM floodplain shows an alluvial unit ranging from 0.70 to 1.95 m in thickness (Figure 4 (RM-UP), see Supplementary material: Figure A for RM-DS). Despite much heterogeneity in the subunit assemblages, the logs from the floodplain generally show fine sand, grading into medium to coarse sand with woody deposits. Some morphological features show active erosional or depositional surfaces, which suggest recent surficial floods. The regional unit forming the left hillslope of the RM stream reveal alternating medium sand and clayey silt deposits of varying thickness, also described as shallow marine surficial deposit from the St. Lawrence Lowlands. The floodplain is embedded in the same regional unit. At the RM-UP site (Figure 4), a very hard clayey matrix is found beneath the regional unit in the right hillslope. The alluvial material of the right end portion of the left floodplain as well as the right floodplain is embedded in the same material, described as glacial till (Ministère des Ressources naturelles et de la Faune du Québec, 2012). The average hydraulic conductivity values for the medium sand and clayey silt regional units and for the alluvial units are 2.61×10^{-5}, 2.46×10^{-7} and 1.96×10^{-5} m/s, respectively.

Figure 4.

3.2 Piezometric Head

3.2.1 Flood periods

For hydrological events occurring during the flood periods, the range of average MCCC values for all the piezometers located in the historic floodplain at the PB and RM sites is between 0.78 and 0.98 (Figure 5, row 1). Not surprisingly, the average MCCC values generally decrease with distance from the stream. These values indicate that the shape of the hydrograph of piezometers located near the stream limit is more similar to the stream hydrograph than those of piezometers near the lateral limit (near the hillslope). This is coherent with the higher average amplitude ratio values (close to 1) measured closer to the stream limit of the historical floodplain than closer to the lateral limit (Figure 5, row 3). The average time lags values between -4 and 6 hours, with the lowest (negative) values generally observed near the lateral limit of the floodplain at all sites (Figure 5, row 2). These relatively small time lags reveal quasi-synchronous fluctuations throughout the entire historic floodplain during hydrological events, with slightly prior response near the lateral limit compared to the fluctuations in the channel. Piezometers located outside the floodplain generally shows the lowest MCCC and amplitude ratio values and highly variable lag time and duration ratio values.

Figure 5.

Results from the PB and RM-UP sites suggest that during a hydrological event, the piezometers located in the abandoned meander (green squares in Figure 5) generally react before (shorter time lags) those situated at a similar distance to the channel but outside the abandoned meander (Figure 5, rows 2), although due to the large time lag variability, these differences are not statistically significant. Moreover, at the RM-Up site, the left floodplain (where the abandoned meander is located) shows higher average MCCC and lower average time lags than the opposite (right) floodplain (Figure 5, rows 1 and 2).

Observations of seasonal water level patterns suggest that the hydraulic gradient in the PB and RM floodplains remains predominantly oriented toward the channel during the entire flood periods when water levels in the channel remain below bank level (Figure 6A, see Supplementary material Figure B, C). On some occasions at PB, at the onset of a hydrological event, a slightly inverted hydraulic gradient develops between the groundwater level in the piezometers close to the channel and those located near the hillslope (Figure 7). Overbank flood events only occur on few occasions (in early spring at PB, in spring and fall at RM). At PB, overbank floods are limited to narrow strips near the stream, as illustrated by maximum values exceeding surface elevation in Figure 6B. At RM, overbank flood events systematically cover the entire historic floodplain (Supplementary material: Figure B and C). During the entire flood period at the PB and RM sites, water levels in the hillslope remain constant and exceed the heads in the nearest floodplain piezometer by at least 0.5 m (Figure 6A, Supplementary material: Figure B and C). The only exception is the RM-UP right hillslope where no water was ever detected in the piezometer.

Figure 6:

Observations of piezometric patterns at the seasonal scale also suggest that the water table near the abandoned meander apex remains generally nearer the floodplain surface than elsewhere at similar distance from the channel (Figure 6B). At RM-UP left and RM-DS (Supplementary material: Figure B and C), the water table depth around the apex of the abandoned meanders remains near zero throughout the flood period. At PB, this pattern is particularly clear in the early spring period for piezometers located near the lateral limit of the floodplain and inside the abandoned meander (M_16 and M_23, green lines in Figure 7) which maintain higher head elevation than piezometers located just outside (M_18 and M_21, yellow lines in Figure 7). It is also notable that during the late spring flood period (mid-April to mid-May) at PB, the amplitude of fluctuations observed near the abandoned meander apex (M_16 and M_23) during hydrological events are much higher than those observed in the piezometers (M_18 and M_21) outside

the abandoned meander (Figure 7). These patterns coincide with the initiation of a head decrease in the hillslope, leading to the low flow period.

Figure 7.

3.2.2 Low-flow period

For hydrological events occurring during the low-flow period, lower values of MCCC are generally observed in the historic floodplain than during the flood periods (Figure 5 and 8, row 1). The most obvious difference between the flood period and the low flow period is observed in the piezometers located near the actual channel at the RM-UP site with the highest average MCCC values measured closer to the hillslope, unlike the PB site (Figure 8, row 1). The same difference between sites applies to the amplitude of head fluctuations with the amplitude ratio at PB generally much lower near the lateral limit of the floodplain during the low-flow period (Figure 8, row 3), indicating fluctuations with relatively small amplitude compared to those close to the channel. Unlike PB, the average peak amplitude ratio at RM is higher close to the lateral limit of the floodplain than close to the stream (Figure 8, row 3).

At the RM sites, piezometers located in the abandoned meander exhibit the highest amplitude among all piezometers (green squares in Figure 8, row 3). Results at RM also suggest that the relative duration of hydrological events is shorter in piezometers located in the abandoned meander (Figure 8, row 4). Among all the sites, the average time lags oscillate between −8.5 and 10.8 h (Figure 8, row 2), with less contrast for piezometers located within the abandoned meander than piezometers located outside the abandoned meander compared with the flood period.

Figure 8.

The hydraulic gradient at all sites during the low-flow period is generally stream oriented (Figure 9, see Supplementary material D and E). At PB, short-duration gradient inversion occurs between the stream

296 and the piezometers close to the channel due to a slight delay between the head response in the
297 piezometers near the channel and the fluctuation in the channel. This contrasts with the flood period
298 where a hydraulic gradient inversion only occurred during overbank channel events. By the end of the
299 summer at PB, groundwater levels eventually decrease below the piezometer, resulting in a net decrease
300 of hydraulic gradients. At the RM sites, the decrease of the head on the hillslope never exceeded 1 m
301 (Supplementary material: Figure E and F). Unlike PB, a strong hydraulic gradient from the hillslope to the
302 floodplain thus remained throughout the study period. No overbank event occurred at both sites during
303 the entire low-flow period (Figure 9B). However, at the RM sites, water table elevations occasionally
304 reached the surface elevation of the floodplain, specifically at the location of the abandoned meander
305 apex (Supplementary material: Figure E and F).

306 **Figure 9.**

307 # 4. DISCUSSION
308

309 ## 4.1 The challenges of understanding subsurface hydrological processes in degraded alluvial
310 environments
311

312 To the best of our knowledge, this study presents a first attempt to document with such high
313 spatiotemporal resolution the groundwater-surface water interactions between straightened reaches and
314 their historical floodplain and adjacent hillslopes. There are many challenges associated with the
315 interpretation of these new data, in particular in terms of statistical analyses due to the intrinsically high
316 level of variability in piezometric data in these complex degraded environments. Floodplain piezometers
317 represent head fluctuations in a transitional geological area connecting surface water in the channel with
318 the regional aquifer (Cranswick et al. 2015). This transitional area is subject to external controls such as
319 stream water level and hillslope heads, precipitation and evapotranspiration. These controls can mask the
320 influence of parameters intrinsic to the floodplain, such as effective porosity of the geological material,

and morphology and stratigraphy of the deposits. This combination of influences can result in a high spatiotemporal variability of the piezometric response within the floodplain and increases the challenge of identifying significant differences in head fluctuation patterns at a given site.

Results from this study converge to support the idea that straightened lowland streams can still be hydrologically connected to their historic floodplain. For example, the generally high MCCC values and low time lag values indicate strong synchronicity between fluctuations in straightened lowland rivers and those in their historic floodplain. In addition, our findings provide evidence that abandoned meanders have a higher level of hydrological connectivity within the floodplains. This is particularly evident when events are analysed independently of each other. For example, the hydrograph for the event of August 8, 2019, at RM-UP (Figure 10) reveals that most fluctuations recorded in the floodplain were concentrated around the abandoned meander apex and near the hillslope (left and right), and that these fluctuations occurred slightly before those in the piezometers near the channel.

Figure 10.

4.2 Conceptual Model of Hydrologic Connectivity in Straightened Lowland Headwater Streams

4.2.1 Hydrological controls

The combination of groundwater flows from the hillslope and the transient bank storage originating from the channel during a hydrological event are the main processes that appear to influence piezometric fluctuations in the floodplain of straightened lowland headwater streams. These original results contribute to better conceptualize the role of the floodplain in maintaining hydrologic connectivity between an agricultural stream and the neighboring aquifer (Figure 11). During the flood and low-flow periods at all three studied straightened meanders, stream stage fluctuations modify the hydraulic gradient between the stream and the floodplain. During the rising limb, the stream-oriented hydraulic gradient either decreases (Figure 11, point 1), which can induce the propagation of a pressure wave away

from the channel (Lewandowski et al., 2009; Buffin-Bélanger et al., 2016), or is temporarily inverted (Figure 11, point 2), potentially resulting in subsurface flows toward the floodplain (Winter, 1999; Flipo et al., 2014). Relatively rapid increases of piezometric levels in each studied floodplain reach, driven by stream stage fluctuations, are interpreted as transient bank storage (Cranswick & Cook, 2015; Winter, 1999).

The presence of higher heads in the hillslope at each study site can also control piezometric fluctuations in the historic floodplain of the straightened channels (Figure 11, point 3). At the RM sites, the relatively high hydraulic conductivity of the hillslope material probably contributed to higher hillslope heads and probably indicate groundwater flow toward the lateral limit of the floodplain (Vidon & Hill, 2004; Jencso et al., 2010). At PB, given the low hydraulic conductivity of the hillslope material, the elevated heads could result in limited groundwater flow between the hillslope and the alluvial deposits, especially during the flood period. The overall shorter time lags calculated in the piezometers located near the hillslope compared to those at the stream limit illustrate that flows originating from the hillslope and the channel are not of the same magnitude and are potentially not perfectly synchronized during a hydrological event. The only exceptions, when all floodplain piezometers fluctuate synchronously with the stream stage, occur during overbank flooding events (Figure 11, point 4). However, complete flooding of the floodplain only occurred at the RM sites, as the backfilling of the floodplain at the PB site considerably limits the extent of overbank flooding (Figure 11, point 5). Otherwise, with the dominant hydraulic gradient oriented towards the stream, groundwater likely flows from the lateral limit to the stream limit of the floodplain (Figure 11, point 6).

During a hydrological event, both elevated heads in the hillslope and stream stage fluctuations thus contribute to a high level of hydrological connectivity with the floodplain, resulting in piezometric fluctuations that are larger within the floodplain than in the adjacent hillslope material. The results show

that lag-time values can help differentiate signal propagation of regional groundwater (negative lag) from surface water-groundwater connectivity at the channel-bank interface (positive lag) (Figures 5 and 8).

Additional hydrological factors that may control the degree of correlation between surface water and piezometric fluctuations observed within the floodplain relate to local recharge from precipitation and antecedent head level. In the spring and late-fall flood periods, evapotranspiration over the floodplain should be relatively minimal, which allows precipitation to percolate through the alluvial deposits and induce head fluctuations (Figure 11, point 7). Antecedent high head level in the floodplain and especially along the lateral limit of the floodplain however may limit head fluctuation during hydrological events and affect MCCC values. By midsummer, during low-flow periods, local precipitation has hardly any influence on floodplain heads, as most precipitation is likely intercepted by vegetation or lost by evaporation (Lalot, 2014). At the PB site, the very fine texture of the backfilling unit placed upon the former meandering stream floodplain probably limits percolation, reduces recharge within the floodplain, and limits piezometric fluctuations from vertical inflows (Figure 11, point 8).

4.2.2 Geomorphic controls

The level of hydrologic connectivity between lowland straightened headwater streams, their former floodplain, and their hillslope is not spatially and temporally uniform, even within a given reach. For instance, the right floodplain at the RM-UP site suggests that very low hydraulic conductivity material in the hillslope and basal unit of the floodplain may influence piezometric fluctuations within the floodplain. The compact and low permeability till material on the right-hand hillslope (Figure 4) probably contributes to only very limited seepage toward the floodplain (Figure 11, point 9). The similar material and the configuration of the basal unit material on the right floodplain of the RM-UP site also likely explain why none of the piezometers along this stream limit react during summer hydrological events (Figure 11, point 10). Ultimately, the RM-UP site highlights that marked contrasts in hydrologic connectivity occur at the

scale of two opposing floodplains of the same straightened reach, with one of them comprising an abandoned channel.

Our results suggest that head fluctuations patterns are markedly different at the location of the abandoned meander apex than in the rest of the floodplain in specific hydrological periods. During the flood period, piezometric level near the former meander apex remains high, distinctively from fluctuations in the channel or in the rest of the floodplain. During the transition between flood and low-flow periods, the greatest amplitude of fluctuations along the hillslope during hydrological events is observed in the piezometers located near the abandoned meander apex. At RM, unlike at the PB site, greater piezometric fluctuations around the abandoned meander apex were observed for all low-flow period events, while hillslope heads remained above the adjacent floodplain.

These observations highlight the critical role of the abandoned meander apex in the complex spatiotemporal pattern of hydrologic connectivity observed between the straightened channel, its floodplain, and its hillslope. A higher degree of hydrologic connectivity at the location of the abandoned meander apex stems partially from the quasi-simultaneous but opposite pressure pulses from hillslope recharge and streamflow, although it remains difficult to identify the specific contribution of each process in the context of this study. Nevertheless, changes in the hydraulic gradient between the stream, the floodplain, and the hillslope as well as the hydraulic conductivity of the hillslope material and the antecedent floodplain heads cannot themselves explain the distinct piezometric fluctuation patterns observed near the abandoned meander apex.

Like their natural counterpart, abandoned meanders resulting from channel straightening potentially form surficial depressions within the floodplain. The lowest area of these abandoned channels generally corresponds to the apex of meanders where there used to be a pool. At the scale of one straightened meander, the former apex zone can converge surficial runoff from the adjacent hillslope (Figure 11, point

11) and from the surrounding floodplain (Figure 11, point 12) following a precipitation event (Mertes, 1997). At the RM sites, for instance, the surface depressions at the apex of the abandoned meander can still be observed and likely contribute to surface runoff toward these specific areas of the floodplain. The bottom contact of the alluvial floodplain material also generally displays an asymmetric and concave morphology, with a depression likely to form at the apex of meander bends toward which groundwater can be temporarily oriented during hydrological events, therefore contributing to a larger amplitude of piezometric fluctuations in the apex of the abandoned meander (Figure 11, point 13) (Ali et al., 2011). It is also likely that the coarser material and the woody deposits associated with the former channel apex, as observed at the PB site, define high conductivity facies and therefore act on preferential flow paths, as suggested in lowland environment (Duval & Hill, 2006; Welch et al., 2014; Wallace & Soltanian, 2021).

Figure 11.

Because the experimental setting measured hydraulic heads, the results of this study only infer pressure exchanges and not directly hydrological fluxes. Also, with the available data, it is not possible to differentiate between precipitation events that occur at the study sites from those that occur upstream. Moreover, our findings must be interpreted in the context of straightened streams in lowland settings. In other settings, for example in a piedmont environment, hydrologic connectivity of straightened streams may differ. Nevertheless, it is worth noting that subsurface pressure transfers operating between the straightened stream and the stream limit of the floodplain, and between the hillslopes and the lateral limit of the floodplain, remain active at least for part of the year, which contrasts with findings by Lewandowski et al. (2009) in an abandoned meander of the lowland River Spree (Germany). This connectivity varies in time and space depending on the texture and configuration of the floodplain and hillslope material, the orientation and magnitude of the hydraulic gradients, and the antecedent saturation conditions, as observed in natural meandering lowland streams (Boulton et al., 1998; Cranswick & Cook, 2015; Biehler et al., 2020).

4.3 Implications for restoration planners and stakeholders

Increasingly, institutional and government stakeholders are raising concerns about the consequences of high levels of disturbance in low-order agricultural streams, resulting in rapid ecological degradation (Vidon & Hill, 2004; Colvin et al., 2019). Given their small drainage area and the absence of cumulative upstream sources of disturbance, headwater streams have greater potential to recover naturally from ecological degradation than higher-order streams. Headwater streams in agricultural setting are thus ideal sites for the restoration of ecological services that are likely to benefit at the watershed scale (Lowe & Likens, 2005; Nadeau & Rains, 2007; Creed et al., 2017; Schilling et al., 2018). Our results indicate that despite intense morphological perturbations, the historic floodplains of straightened headwater streams act as preferential areas of hydrologic connectivity in an agricultural lowland environment. While backfill material placed upon the floodplain limits the extent of surficial flooding, it appears they have no substantial effect on subsurface hydrologic connectivity. These findings thus provide useful arguments to put in place restoration programs targeting these environments.

This study also highlights that it is possible to interpret head fluctuations within historic floodplains of straightened headwater streams based on the pre-disturbance geomorphological configuration of these environments, as proposed by Larocque et al. (2016). Understanding the nature of deposits and the hydrogeomorphological components (e.g., historical position of meanders and hillslopes) can help restoration planners classify the historic floodplains and the abandoned meanders according to their potential level of hydrologic connectivity. Using LiDAR images, historical photos, and maps of surface deposits, restoration planners can delineate, throughout a watershed, areas of strong hydrologic connectivity surrounding the apex of ancient meanders, along straightened headwater streams in agricultural environments.

Knowing areas of high hydrologic connectivity allows restoration projects to better align with the ecological services targeted for restoration (Phillips, 2013). For example, results from this study suggest that the transient water storage in the historical floodplain of straightened streams occurs during hydrological events. Therefore, active restoration measures such as removing backfilling material above abandoned meanders (cf. PB site) or removing embankments (Addy & Wilkinson, 2021) represent potential means of increasing water storage during hydrological events and can therefore contribute to flow regulation by reducing peak streamflow. Integrating the specific configuration of the historical floodplain in the planning of riparian buffers could also help improve their effectiveness in intercepting agrochemical pollution (Kaushal et al., 2008; Hénault-Ethier et al., 2017). The presence of revegetation at the RM site illustrates that, in the absence of floodplain backfilling and with a regional aquifer highly connected to the floodplain through the hillslope, passive restoration of the historic floodplain can lead to the recovery of various types of riparian wetlands. Evidently, for this passive restoration to significantly impact flow regulation, pollutant control, habitat diversification, and recreational uses at the watershed scale, many abandoned meanders along straightened channels must be restored.

However, large-scale restoration measures providing sufficient space for hydrogeomorphological processes to operate (e.g. Kondolf, 2012; Biron et al., 2014; Massé et al., 2020) can be complex in the context of lowland agricultural watersheds with many landowners along a given reach. As key residual components of the hydrologic connectivity of straightened headwater streams, the artificially abandoned meanders could be used to develop floodplain restoration strategies adapted to the scale of the land owned by farmers. Abandoned meanders are distinct, relatively small, and easily identifiable physical spaces that facilitate discussions with landowners to better understand the purpose of a restoration project. From a social acceptability perspective, it is also easier to initiate a restoration project at this scale than to limit agricultural activities indiscriminately along complete portions of a stream. An abandoned

meander of a degraded agricultural stream is therefore an excellent "feature" to popularize the concept of hydrologic connectivity in its simplest expression.

5. CONCLUSION

Like their lowland meandering stream counterparts, alluvial deposits that form the historic floodplain of straightened streams act as a continuum zone connecting surface water to shallow regional groundwater. Our high-resolution spatiotemporal piezometric dataset suggests that the abandoned meanders and, more specifically, their apex, exhibit a higher level of hydrologic connectivity than the rest of the historical floodplain. The hydrogeomorphological configuration of the former meanders, with a marked surface and subsurface depression at the meander apex, results in a convergence of hydrological flows from the hillslopes and the rest of the floodplain toward the apex zones during hydrological events.

Our findings suggest that the degree of alteration of subsurface hydrological exchanges in straightened lowland streams is relatively low compared with surface exchanges adversely impacted by channel incision and floodplain backfilling. It therefore follows that despite a drastic change in channel morphology and the floodplain features that limits surface exchanges, a straightened stream presents head fluctuation patterns within its historical floodplain that are relatively similar to those in a meandering lowland stream during hydrological events when the water level remains below bank level. It is reasonable to assume that the same potential to form diverse and sustainable riparian habitats in former meanders of straightened streams is similar to that of natural abandoned meanders. The Ruisseau Martin site provides useful evidence of this, with its abandoned meanders occupied by forested and shrub swamp and herbaceous marshes (unpublished data on vegetation surveys). There is therefore more than meets the eye in these degraded environments.

Further studies should focus on water exchanges operating within straightened streams, their historic floodplain, and the hillslopes at different spatial scales and under various hydrological regimes. Relevant

questions need to be investigated concerning the role of local hydrological exchanges or pressure transfers in terms of surface water temperature regulation, solute transformation, and discharge regulation at the watershed scale. For example, it would be insightful to quantify transient water storage in the different apex zones bordering a straightened lowland stream at the scale of a predominantly agricultural watershed. Hydrogeological or hydrogeochemical modelling of abandoned channels in lowland agricultural settings could potentially identify restoration approaches, active or passive, that maximize the functions of water storage and nutrient fixation. Filling this knowledge gap might contribute to help counter the rapid ecological degradation of agricultural watersheds in lowland settings by restoring ecological processes in their headwater streams (Lowe & Likens, 2005; Schilling et al., 2018). Developing restoration approaches centered around the remaining hydrologic connectivity occurring in these streams floodplains appears essential to increase their natural resilience, since they often lack the stream power to recover sediment-transport processes (Brookes, 1987; Kondolf, 2012; Kristensen et al., 2013).

With increased access to LiDAR data, combined with the analysis of historical aerial photos and surface deposits, it is possible to delimit historical floodplains of straightened lowland headwater streams and use this information as a critical first step in planning restoration strategies at the watershed scale. Where social acceptability exists among agricultural producers, it may then be possible to put forward a restoration plan for these streams, one abandoned meander at a time.

REFERENCES

Addy, S., & Wilkinson, M. E. (2021). Embankment lowering and natural self-recovery improves river-floodplain hydro-geomorphic connectivity of a gravel bed river. *Science of The Total Environment*, *770*, 144626.

Ali, G. A., L'heureux, C., Roy, A. G., Turmel, M., & Courchesne, F. (2011). Linking spatial patterns of perched groundwater storage and stormflow generation processes in a headwater forested catchment. *Hydrological Processes*, *25*(25), 3843–3857.

Beechie, T. J., Sear, D. A., Olden, J. D., Pess, G. R., Buffington, J. M., Moir, H., Roni, P., & Pollock, M. M. (2010). Process-based principles for restoring river ecosystems. *Bioscience*, *60*(3), 209–222.

Biehler, A., Chaillou, G., Buffin-Bélanger, T., & Baudron, P. (2020). Hydrological connectivity in the aquifer–river continuum: Impact of river stages on the geochemistry of groundwater floodplains. *Journal of Hydrology*, *590*, 125379.

Biron, P. M., Buffin-Bélanger, T., Larocque, M., Choné, G., Cloutier, C.-A., Ouellet, M.-A., Demers, S., Olsen, T., Desjarlais, C., & Eyquem, J. (2014). Freedom space for rivers: A sustainable management approach to enhance river resilience. *Environmental Management*, *54*(5), 1056–1073.

Boulton, A. J. (2007). Hyporheic rehabilitation in rivers: Restoring vertical connectivity. *Freshwater Biology*, *52*(4), 632–650. https://doi.org/10.1111/j.1365-2427.2006.01710.x

Boulton, A. J., Findlay, S., Marmonier, P., Stanley, E. H., & Valett, H. M. (1998). The functional significance of the hyporheic zone in streams and rivers. *Annual Review of Ecology and Systematics*, *29*(1), 59–81.

Brookes, A. (1987). Restoring the sinuosity of artificially straightened stream channels. *Environmental Geology and Water Sciences*, *10*(1), 33–41. https://doi.org/10.1007/BF02588003

Buffin-Bélanger, T., Biron, P. M., Larocque, M., Demers, S., Olsen, T., Choné, G., Ouellet, M.-A., Cloutier, C.-A., Desjarlais, C., & Eyquem, J. (2015). Freedom space for rivers: An economically viable river management concept in a changing climate. *Geomorphology*, *251*, 137–148.

551 Buffin-Bélanger, T., Cloutier, C.-A., Tremblay, C., Chaillou, G., & Larocque, M. (2016). Dynamics of
552 groundwater floodwaves and groundwater flood events in an alluvial aquifer. *Canadian Water*
553 *Resources Journal*, *41*(4), 469–483. https://doi.org/10.1080/07011784.2015.1102651
554 Clilverd, H. M., Thompson, J. R., Heppell, C. M., Sayer, C. D., & Axmacher, J. C. (2013). River–floodplain
555 hydrology of an embanked lowland Chalk river and initial response to embankment removal.
556 *Hydrological Sciences Journal*, *58*(3), 627–650.
557 Colvin, S. A., Sullivan, S. M. P., Shirey, P. D., Colvin, R. W., Winemiller, K. O., Hughes, R. M., Fausch, K. D.,
558 Infante, D. M., Olden, J. D., & Bestgen, K. R. (2019). Headwater streams and wetlands are critical
559 for sustaining fish, fisheries, and ecosystem services. *Fisheries*, *44*(2), 73–91.
560 Cranswick, R. H., & Cook, P. G. (2015). Scales and magnitude of hyporheic, river–aquifer and bank
561 storage exchange fluxes. *Hydrological Processes*, *29*(14), 3084–3097.
562 Creed, I. F., Lane, C. R., Serran, J. N., Alexander, L. C., Basu, N. B., Calhoun, A. J., Christensen, J. R., Cohen,
563 M. J., Craft, C., & D'Amico, E. (2017). Enhancing protection for vulnerable waters. *Nature*
564 *Geoscience, 10, Doi:10.1038/NGEO3041*.
565 D'Ambrosio, J. L., Williams, L. R., Williams, M. G., Witter, J. D., & Ward, A. D. (2014). Geomorphology,
566 habitat, and spatial location influences on fish and macroinvertebrate communities in modified
567 channels of an agriculturally-dominated watershed in Ohio, USA. *Ecological Engineering*, *68*, 32–
568 46.
569 Devlin, J. F. (2015). HydrogeoSieveXL: an Excel-based tool to estimate hydraulic conductivity from grain-
570 size analysis. *Hydrogeology Journal*, *23*(4), 837–844.
571 Duval, T., & Hill, A. (2006). Influence of stream bank seepage during low-flow conditions on riparian zone
572 hydrology. *Water Resources Research*, *42*(10), W10425.

573 Flipo, N., Mouhri, A., Labarthe, B., Biancamaria, S., Rivière, A., & Weill, P. (2014). Continental
574 hydrosystem modelling: The concept of nested stream–aquifer interfaces. *Hydrology and Earth*
575 *System Sciences*, *18*(8), 3121–3149.
576 Franklin, S. B., Kupfer, J. A., Pezeshki, S. R., Gentry, R., & Smith, R. D. (2009). Complex effects of
577 channelization and levee construction on western Tennessee floodplain forest function.
578 *Wetlands*, *29*(2), 451–464. https://doi.org/10.1672/08-59.1
579 Graf, W., Leitner, P., Hanetseder, I., Ittner, L., Dossi, F., & Hauer, C. (2016). Ecological degradation of a
580 meandering river by local channelization effects: A case study in an Austrian lowland river.
581 *Hydrobiologia*, *772*(1), 145–160.
582 Gumiero, B., Mant, J., Hein, T., Elso, J., & Boz, B. (2013). Linking the restoration of rivers and riparian
583 zones/wetlands in Europe: Sharing knowledge through case studies. *Ecological Engineering*, *56*,
584 36–50.
585 Hénault-Ethier, L., Larocque, M., Perron, R., Wiseman, N., & Labrecque, M. (2017). Hydrological
586 heterogeneity in agricultural riparian buffer strips. *Journal of Hydrology*, *546*(Supplement C),
587 276–288. https://doi.org/10.1016/j.jhydrol.2017.01.001
588 Hester, E. T., & Gooseff, M. N. (2010). *Moving beyond the Banks: Hyporheic Restoration Is Fundamental*
589 *to Restoring Ecological Services and Functions of Streams*. *Environmental Science & Technology*,
590 44(5), 1521-1525.
591 Hupp, C. R. (1992). Riparian vegetation recovery patterns following stream channelization: A
592 geomorphic perspective. *Ecology*, *73*(4), 1209–1226.
593 Hvorslev, M. J. (1951). *Time lag and soil permeability in ground-water observations*. Waterways Exper.
594 Sta. Corps of Engrs, U.S. Army, Vicksburg.
595 Jencso, K. G., McGlynn, B. L., Gooseff, M. N., Bencala, K. E., & Wondzell, S. M. (2010). Hillslope
596 hydrologic connectivity controls riparian groundwater turnover: Implications of catchment

structure for riparian buffering and stream water sources. *Water Resources Research*, *46*(10), 2009WR008818.

Käiro, K., Haldna, M., Timm, H., & Virro, T. (2017). The effect of channelization on the biological quality of lowland streams using macroinvertebrates as proxies. *Hydrobiologia*, *794*(1), 167–177.

Kasahara, T., & Hill, A. R. (2006). Hyporheic exchange flows induced by constructed riffles and steps in lowland streams in southern Ontario, Canada. *Hydrological Processes: An International Journal*, *20*(20), 4287–4305.

Kaushal, S. S., Groffman, P. M., Mayer, P. M., Striz, E., & Gold, A. J. (2008). Effects of stream restoration on denitrification in an urbanizing watershed. *Ecological Applications*, *18*(3), 789–804.

Kondolf, Boulton, A., O'Daniel, S., Poole, G., Rahel, F., Stanley, E., Wohl, E., Bång, A., Carlstrom, J., & Cristoni, C. (2006). Process-based ecological river restoration: Visualizing three-dimensional connectivity and dynamic vectors to recover lost linkages. *Ecology and Society*, *11*(2).

Kondolf, G. M. (2012). The Espace de Liberté and restoration of fluvial process: When can the river restore itself and when must we intervene? *River Conservation and Management*, 225–242.

Kristensen, E. A., Thodsen, H., Dehli, B., Kolbe, P. E. Q., Glismand, L., & Kronvang, B. (2013). Comparison of active and passive stream restoration: Effects on the physical habitats. *Geografisk Tidsskrift-Danish Journal of Geography*, *113*(2), 109–120.

Lalot, E. (2014). *Analyse Des Signaux Piezométriques et Modélisation Pour l'évaluation Quantitative et La Caractérisation Des Échanges Hydrauliques Entre Aquifères Alluviaux et Rivières-Application Au Rhône.* Sciences de la Terre. École nationale Supérieure des Mines de Saint-Etienne, 2014. Français

Larocque, M., Biron, P. M., Buffin-Bélanger, T., Needelman, M., Cloutier, C.-A., & McKenzie, J. M. (2016). Role of the geomorphic setting in controlling groundwater–surface water exchanges in riverine

wetlands: A case study from two southern Québec rivers (Canada). *Canadian Water Resources Journal*, *41*(4), 528–542. https://doi.org/10.1080/07011784.2015.1128360

LaSage, D. M., Sexton, J. L., Mukherjee, A., Fryar, A. E., & Greb, S. F. (2008). Groundwater discharge along a channelized Coastal Plain stream. *Journal of Hydrology*, *360*(1–4), 252–264. https://doi.org/10.1016/j.jhydrol.2008.06.026

Lewandowski, J., Lischeid, G., & Nützmann, G. (2009). Drivers of water level fluctuations and hydrological exchange between groundwater and surface water at the lowland River Spree (Germany): Field study and statistical analyses. *Hydrological Processes*, *23*(15), 2117–2128.

Liu, X., Vidon, P., Jacinthe, P.-A., Fisher, K., & Baker, M. (2014). Seasonal and geomorphic controls on N and P removal in riparian zones of the US Midwest. *Biogeochemistry*, *119*(1), 245–257.

Lowe, W. H., & Likens, G. E. (2005). Moving headwater streams to the head of the class. *Bioscience*, *55*(3), 196–197.

Massé, S., Demers, S., Besnard, C., Buffin-Bélanger, T., Biron, P. M., Choné, G., & Massey, W. (2020). Development of a mapping approach encompassing most fluvial processes: Lessons learned from the freedom space for rivers concept in Quebec (Canada). *River Research and Applications*, *36*(6), 947–959.

Mertes, L. A. (1997). Documentation and significance of the perirheic zone on inundated floodplains. *Water Resources Research*, *33*(7), 1749–1762.

Ministère des Ressources naturelles et de la Faune du Québec (2012). Cartes numériques des dépôts de surface 1/50 000. http://mffp.gouv.qc.ca/les-forets/inventaire-ecoforestier/

Nadeau, T., & Rains, M. C. (2007). Hydrological connectivity between headwater streams and downstream waters: How science can inform policy. *JAWRA Journal of the American Water Resources Association*, *43*(1), 118–133.

643 Phillips, J. D. (2013). Hydrological connectivity of abandoned channel water bodies on a coastal plain
644 river. *River Research and Applications*, *29*(2), 149–160.
645 Pierce, A. R., & King, S. L. (2017). Hydrological Responses to Channelization and The Formation of Valley
646 Plugs and Shoals. *Wetlands*, *37*(3), 513–523. https://doi.org/10.1007/s13157-017-0886-4
647 Poppe, L. J., Eliason, A. H., Fredericks, J. J., Rendigs, R. R., Blackwood, D., & Polloni, C. F. (2000). Grain
648 size analysis of marine sediments: Methodology and data processing. *US Geological Survey East*
649 *Coast Sediment Analysis: Procedures, Database, and Georeferenced Displays. US Geological*
650 *Survey Open File Report 00-358. Http://Pubs. Usgs. Gov/of/2000/Of00-358*.
651 Rousseau, Y., & Biron, P. M. (2009). Geomorphological impacts of Channel Straightening in an
652 Agricultural Watershed, Southwestern Québec. *Northeastern Geographer*, 1, 91-113.
653 Schilling, K. E., & Jacobson, P. (2014). Effectiveness of natural riparian buffers to reduce subsurface
654 nutrient losses to incised streams. *Catena*, *114*, 140–148.
655 Schilling, K. E., Jacobson, P. J., & Wolter, C. F. (2018). Using riparian Zone scaling to optimize buffer
656 placement and effectiveness. *Landscape Ecology*, *33*(1), 141–156.
657 Schilling, K. E., Li, Z., & Zhang, Y.-K. (2006). Groundwater–surface water interaction in the riparian zone
658 of an incised channel, Walnut Creek, Iowa. *Journal of Hydrology*, *327*(1–2), 140–150.
659 Schilling, K., Zhang, Y., & Drobney, P. (2004). Water table fluctuations near an incised stream, Walnut
660 Creek, Iowa. *Journal of Hydrology*, *286*(1), 236–248.
661 Schumm, S. A., Harvey, M. D., & Watson, C. C. (1984). *Incised channels: Morphology, dynamics, and*
662 *control*. Water Resources Publications.
663 Simon, A. (1989). A model of channel response in disturbed alluvial channels. *Earth Surface Processes*
664 *and Landforms*, *14*(1), 11–26.

Trautman, M. B., & Gartman, D. K. (1974). *Re-evaluation of the effects of man-made modifications on Gordon Creek between 1887 and 1973 and especially as regards its fish fauna*. The Ohio Journal of Science, 74(3), 162-173.

Vidon, P. G., & Hill, A. R. (2004). Landscape controls on nitrate removal in stream riparian zones. *Water Resources Research*, *40*(3), W03201, doi:10.1029/2003WR002473.

Wallace, C. D., & Soltanian, M. R. (2021). Surface water-groundwater exchange dynamics in buried-valley aquifer systems. *Hydrological Processes*, *35*(3), e14066.

Welch, C., Harrington, G. A., Leblanc, M., Batlle-Aguilar, J., & Cook, P. G. (2014). Relative rates of solute and pressure propagation into heterogeneous alluvial aquifers following river flow events. *Journal of Hydrology*, *511*, 891–903.

Winter, T. C. (1999). Relation of streams, lakes, and wetlands to groundwater flow systems. *Hydrogeology Journal*, *7*(1), 28–45.

Wohl, E. (2018). Human Alterations of Rivers. In E. Wohl (Ed.), *Sustaining River Ecosystems and Water Resources* (pp. 59–104). Springer International Publishing. https://doi.org/10.1007/978-3-319-65124-8_3

Wohl, E., Lane, S. N., & Wilcox, A. C. (2015). The science and practice of river restoration. *Water Resources Research*, *51*(8), 5974–5997.

Wyzga, B. (1996). Changes in the magnitude and transformation of flood waves subsequent to the channelization of the Raba River, Polish Carapathians. *Earth Surface Processes and Landforms*, *21*(8), 749–763.

APPENDIX A. SUPPLEMENTARY DATA

Supplementary data to this article can be found online.

FIGURE LEGEND

Figure 1: (A) Location of the Petit-Pot-au-Beurre (PB) site in the St. Lawrence Lowlands (Quebec, Canada), (B) in a vast agricultural zone with several straightened meander streams; (C) Piezometers installed within the abandoned meander, in the historical floodplain and on the adjacent hillslope, where numbers next to letters M, F and O indicate the distance (in m) between the piezometer and the stream; (D) The current crop at the site showing fodder plants.

Figure 2. (A) Location of the Ruisseau Martin (RM) site in the St. Lawrence Lowlands (Quebec, Canada) in (B) an area that was mainly agricultural but (C) which has recently evolved toward agroforestry farming. Piezometers were installed within two abandoned meanders (RM-UP, RM-DS) and on the historical floodplain and the adjacent hillslopes, where numbers next to letters M, F and O indicate the distance (in m) between the piezometer and the stream.

Figure 3. (A) Stratigraphic cross-section profile at PB site. Logs labelled with letter *S* (ex. S_24) were only used for the stratigraphic characterization. Logs labelled with letter *M* (ex. M_5.6) and *O* were also used for piezometer installation. Numbers represent the distance to the stream (in m). Note a vertical exaggeration of 3×. (B) Historical aerial photograph (1965) of the PB site prior to channel straightening, with the position of the actual channel. Red dots indicate the stratigraphic logs that were used to build the cross-section profile.

Figure 4. Stratigraphic cross-section profile at RM-UP site, representing the (A) left and (B) right floodplain (looking downstream). Borehole logs labelled with *S* (ex. S_22) were only used for the stratigraphic characterization. Borehole logs labelled with *M* (ex. M_8), *F*, and *O* were also used for the piezometer installation. Numbers represent the distance to the stream (in m). Note a vertical exaggeration of 4×. (C) Digital elevation model of the RM site, with the position of the former and actual channel. Red dots indicate the stratigraphic logs that were used to build the cross-section profiles.

Figure 5. Cross-correlation analysis (MCCC (maximum cross-correlation coefficient), lag time, rows 1 and 2) and hydrograph characteristics (peak amplitude ratio, peak duration ratio, rows 3 and 4) for piezometers at the (A) PB, (B) RM-UP left, (C) RM-UP right, and (D) RM-DS for the flood periods (early March to mid-May, mid-October to late December). The vertical dashed line represents the lateral limit of the historical floodplain.

715 **Figure 6**: Box plot graphs showing A) hydraulic heads and B) water table depths in PB piezometers for the flood
716 period (mid-March to mid-May and early October to late December). Negative water table depths indicate water
717 level above the surface.

718 **Figure 7**. Hydrograph for the flood period between March 1 and May 15, 2020, at the PB site. Notice the distinct
719 head elevation for the early flood period and the larger amplitude of fluctuations during events in the late flood
720 period for the piezometers located in the abandoned meander apex (green lines) compared with those located at a
721 similar distance but outside the former meander (yellow lines). The top and base of the hillslope are presented as
722 they were before channel straightening and backfilling of the floodplain.

723 **Figure 8**. Cross-correlation analysis (MCCC (maximum cross-correlation coefficient), lag time) and hydrograph
724 characteristics (peak amplitude ratio, peak duration ratio) for all piezometers at all studied sites for the low-flow
725 period (mid-May to mid-October).

726 **Figure 9.** Box plot graphs showing A) hydraulic head elevation and B) water depth of piezometers installed at the PB
727 site for the low flow period (mid-May to early October).

728 **Figure 10**. (A) Hydrograph for the August 8, 2019, hydrological event at the RM-UP site. (B) Piezometric maps
729 representing three stages (pre-event, event peak, and post-event) of the August 8, 2019, event. Note that absolute
730 elevations of hydraulic heads were converted to water depth from the surface before interpolation. Negative
731 values (in the existing channel and in the abandoned channel apex) represent water levels above the ground

732 **Figure 11**. Conceptual model of surface and subsurface hydrological exchange mechanisms operating in
733 straightened agricultural lowland streams: (1) bank transient storage during flood period and (2) during low flow
734 period; (3) subsurface flows from permeable hillslope; (4) overbank flow on the undisturbed and (5) backfilled
735 floodplain; (6) subsurface flows toward the stream limit of the floodplain when the stream-oriented hydraulic
736 gradient re-establishes (7) infiltration into the undisturbed floodplain; (8) limited infiltration into the backfilled
737 floodplain; (9) limited subsurface flows from impermeable hillslope; (10) limited surface-groundwater exchange
738 due to the presence of an impermeable basal unit; (11) surface runoff from the hillslope; (12) surface runoff and
739 (13) subsurface flows from the surrounding floodplain toward the meander apex depression during hydrological

events. Overall, these mechanisms define zones of very high to moderately low hydrologic connectivity within the historical floodplain of straightened streams, with the focal zone being located at the apex of the abandoned meander. Red arrows represent exchange mechanisms directly associated with the presence of the former meander apex.

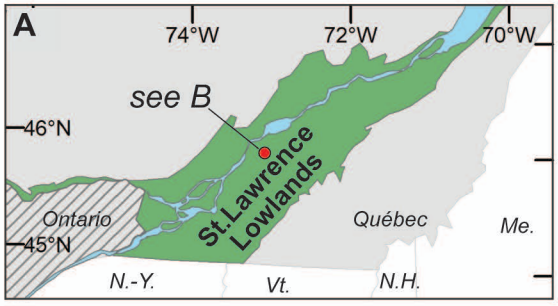

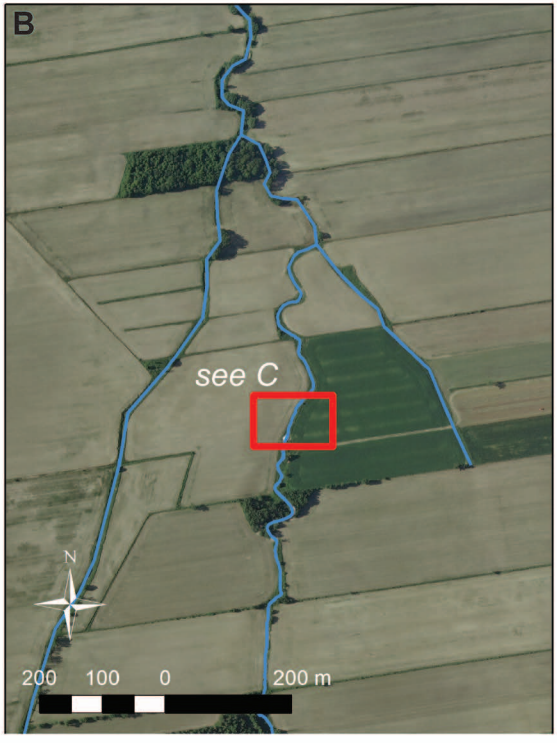

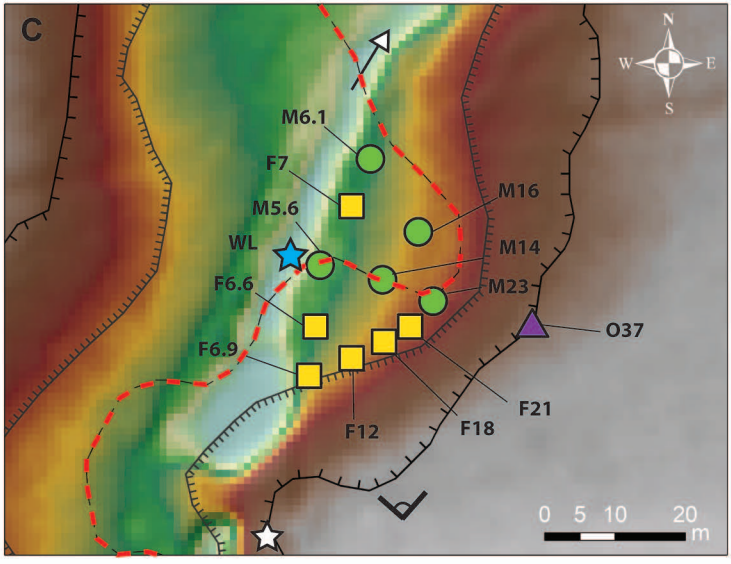

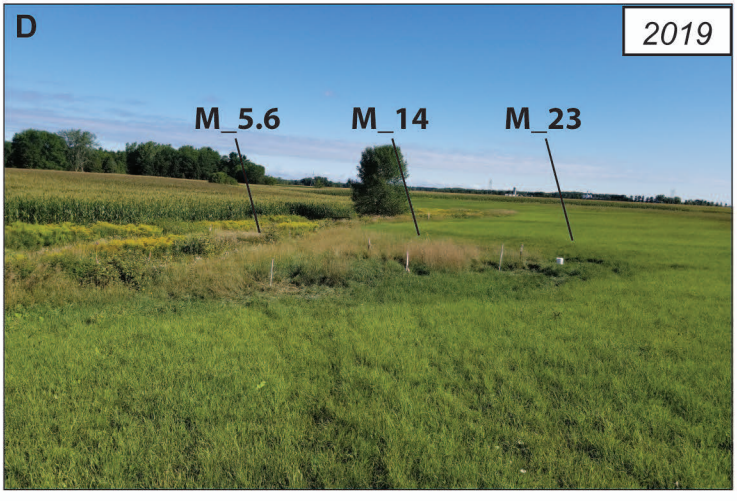

Legend

Piezometers in the abandoned meander	●	*Channel logger:*	★
Piezometers in the floodplain outside the abandoned meander	■	*Barometric logger:*	☆
Piezometers outside the floodplain:	▲	*View angle (D)*	✓

DEM (m. a.s.l.)

High: 18.6

Mid: 17.0

Low: 14.5

- *Actual stream*
- *Top of hillslope (pre-disturbance, 1965)*
- *Base of hillslope (pre-disturbance, 1965)*
- *Abandoned channel*
- *Flow direction*

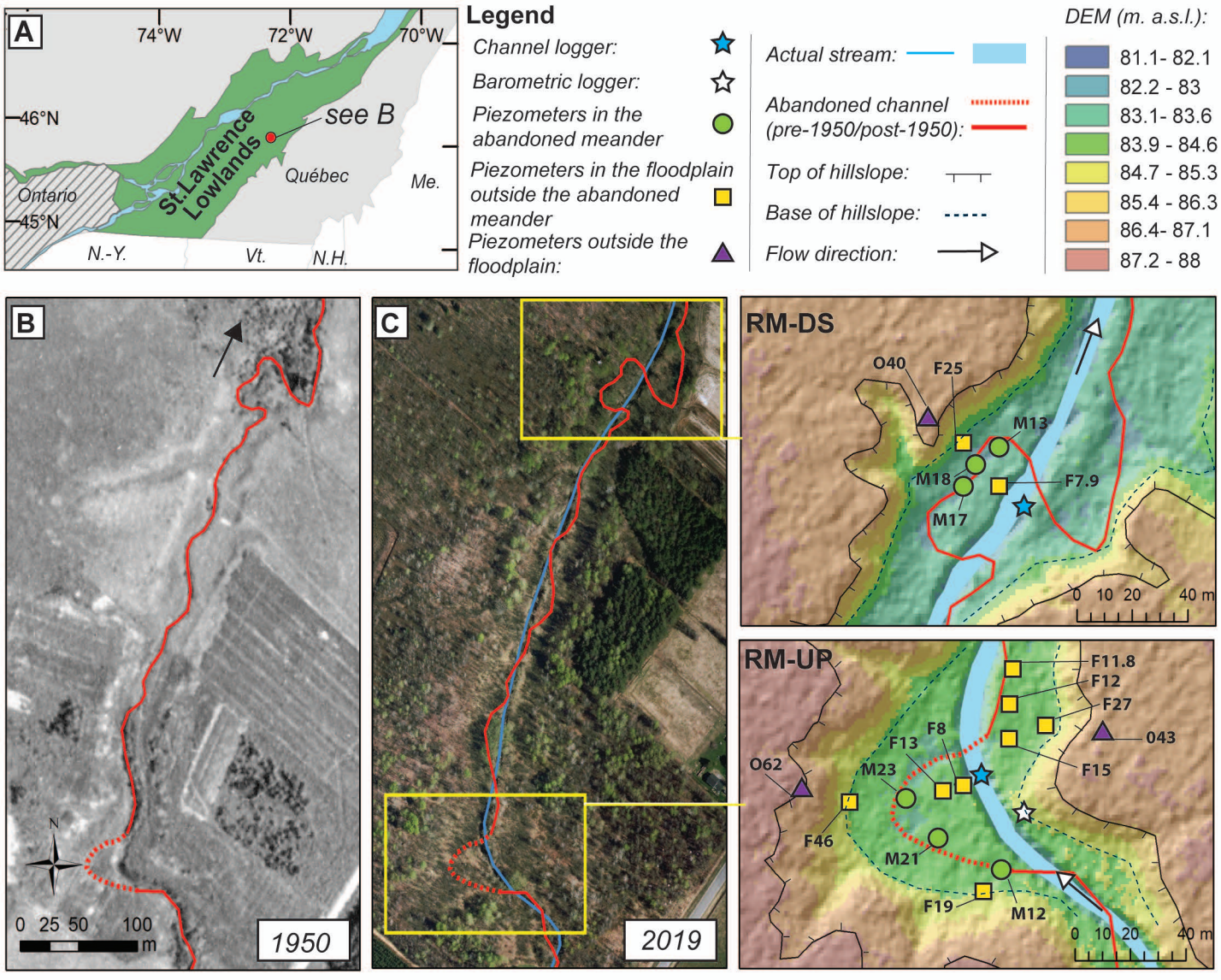
A
74°W
72°W
70°W
46°N
45°N
see B
St.Lawrence Lowlands
Québec
Ontario
Me.
N.-Y.
Vt.
N.H.
Legend
Channel logger:
Barometric logger:
Piezometers in the abandoned meander
Piezometers in the floodplain outside the abandoned meander
Piezometers outside the floodplain:
Actual stream:
Abandoned channel (pre-1950/post-1950):
Top of hillslope:
Base of hillslope:
Flow direction:
DEM (m. a.s.l.):
81.1- 82.1
82.2 - 83
83.1- 83.6
83.9 - 84.6
84.7 - 85.3
85.4 - 86.3
86.4- 87.1
87.2 - 88
B
N
0 25 50 100 m
1950
C
2019
RM-DS
O40
F25
M13
M18
F7.9
M17
0 10 20 40 m
RM-UP
F11.8
F12
F27
043
F8
F13
O62
M23
F15
F46
M21
F19
M12
0 10 20 40 m

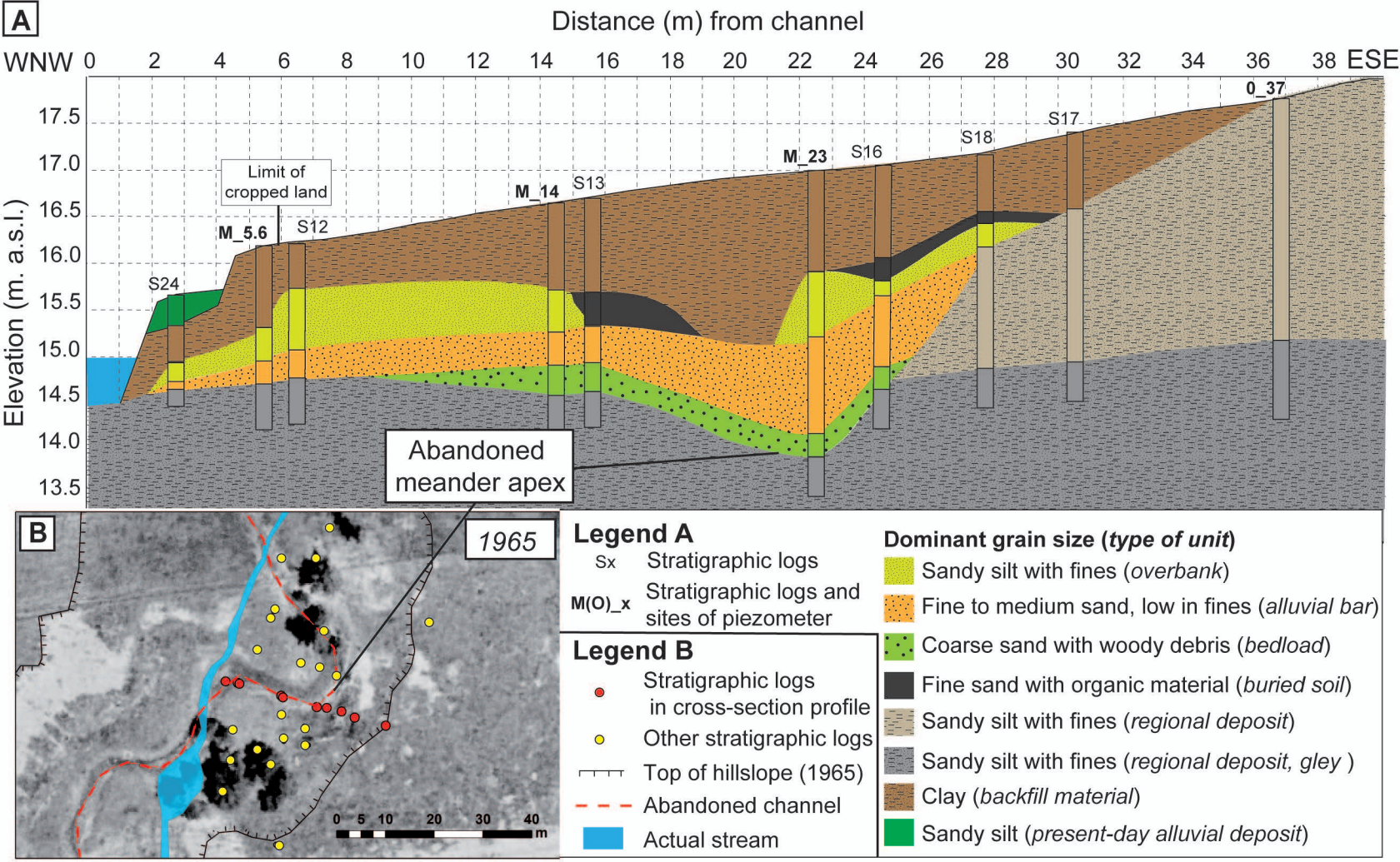
A
Distance (m) from channel
WNW
ESE
0
2
4
6
8
10
12
14
16
18
20
22
24
26
28
30
32
34
36
38
Elevation (m. a.s.l.)
17.5
17.0
16.5
16.0
15.5
15.0
14.5
14.0
13.5
Limit of cropped land
S24
M_5.6
S12
M_14
S13
M_23
S16
S18
S17
0_37
Abandoned meander apex
B
1965
0 5 10 20 30 40 m
Legend A
Sx Stratigraphic logs
M(O)_x Stratigraphic logs and sites of piezometer
Legend B
Stratigraphic logs in cross-section profile
Other stratigraphic logs
Top of hillslope (1965)
Abandoned channel
Actual stream
Dominant grain size (type of unit)
Sandy silt with fines (overbank)
Fine to medium sand, low in fines (alluvial bar)
Coarse sand with woody debris (bedload)
Fine sand with organic material (buried soil)
Sandy silt with fines (regional deposit)
Sandy silt with fines (regional deposit, gley)
Clay (backfill material)
Sandy silt (present-day alluvial deposit)

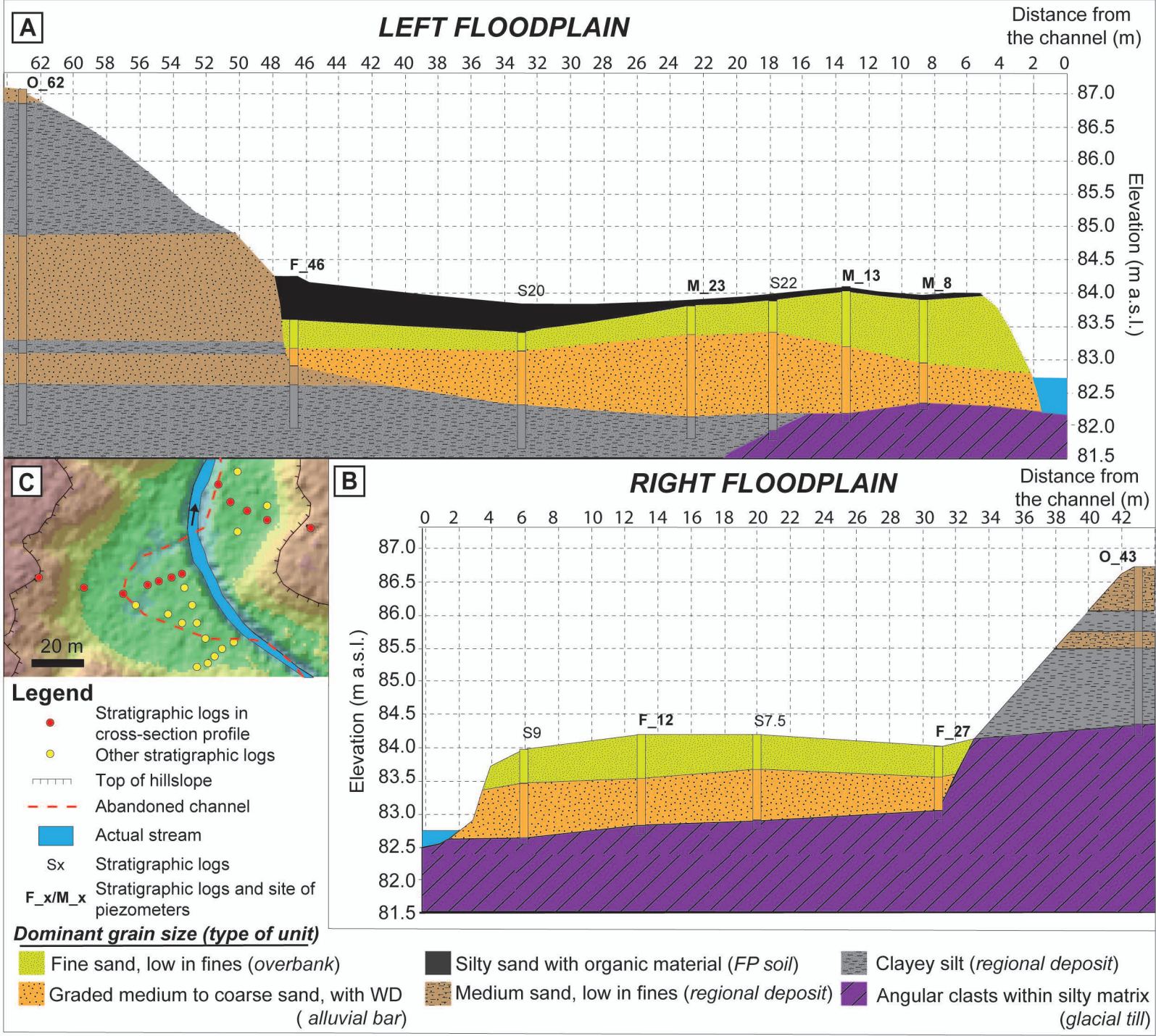
A
LEFT FLOODPLAIN
Distance from the channel (m)
62 60 58 56 54 52 50 48 46 44 42 40 38 36 34 32 30 28 26 24 22 20 18 16 14 12 10 8 6 4 2 0
O_62
F_46
S20
M_23
S22
M_13
M_8
87.0
86.5
86.0
85.5
85.0
84.5
84.0
83.5
83.0
82.5
82.0
81.5
Elevation (m a.s.l.)
C
20 m
B
RIGHT FLOODPLAIN
Distance from the channel (m)
0 2 4 6 8 10 12 14 16 18 20 22 24 26 28 30 32 34 36 38 40 42
O_43
S9
F_12
S7.5
F_27
Elevation (m a.s.l.)
Legend
Stratigraphic logs in cross-section profile
Other stratigraphic logs
Top of hillslope
Abandoned channel
Actual stream
Sx
Stratigraphic logs
F_x/M_x
Stratigraphic logs and site of piezometers
Dominant grain size (type of unit)
Fine sand, low in fines (overbank)
Graded medium to coarse sand, with WD (alluvial bar)
Silty sand with organic material (FP soil)
Medium sand, low in fines (regional deposit)
Clayey silt (regional deposit)
Angular clasts within silty matrix (glacial till)

FLOOD PERIOD EVENTS

Variables	Petit-Pot-au-Beurre	Martin-UP-Left	Martin-UP-Right	Martin-DS
1 Avg MCCC	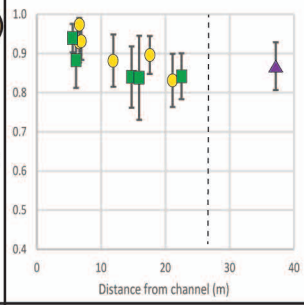	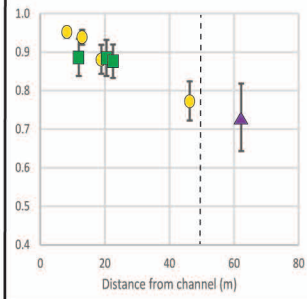	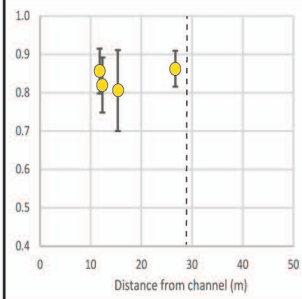	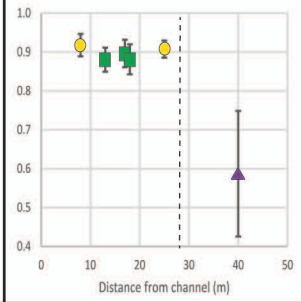
2 Avg Lag	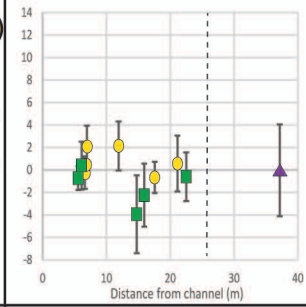	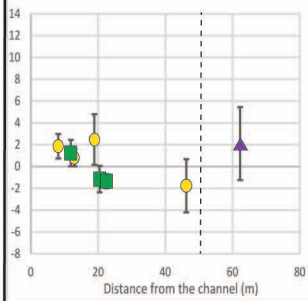	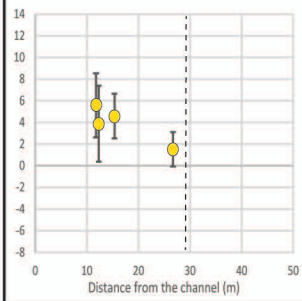	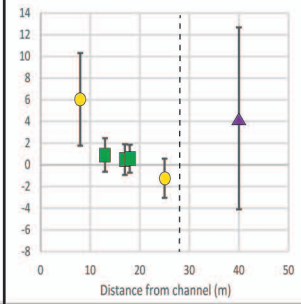
3 Avg amplitude ratio	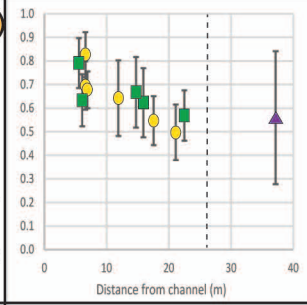	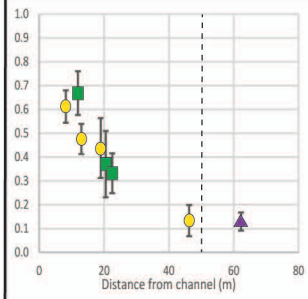	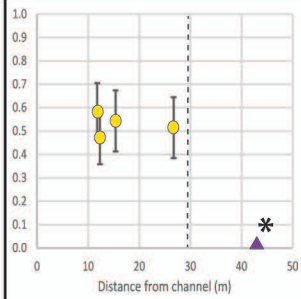	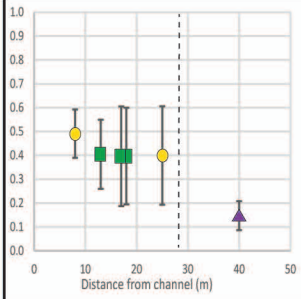
4 Avg duration ratio	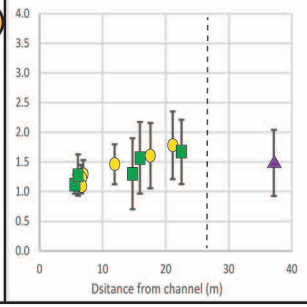	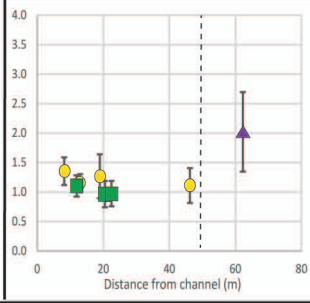	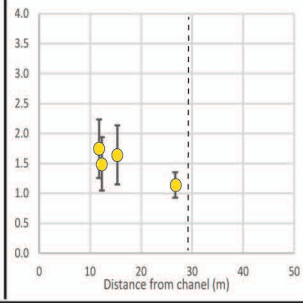	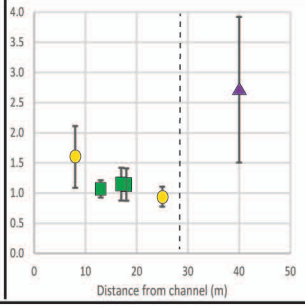

LEGEND: Piezometers located within the abandoned meander; Piezometers in the rest of the floodplain; Piezometers outside the floodplain; Standard error (p-value: 0.95); * No fluctuation recorded (entire study period); Limit of hillslope

Petit-Pot-au-Beurre (PB)-FLOOD PERIOD

A

Hydraulic head (m a.s.l)

WL, M6.1, M5.6, F6.6, F6.9, F7, Dominant hydraulic gradient, F12, M14, M16, F18, F21, M23, O37

Distance from channel (m)

B

Water table depth (m)

OVERBANK FLOW

Surface elevation

M5.6, M6.1, F6.6, F6.9, F7, F12, M14, M16, F18, F21, M23, O37

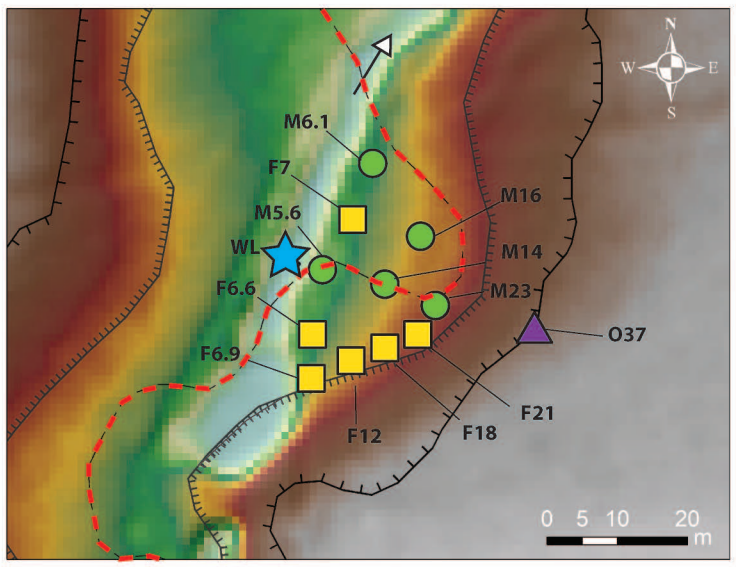

Legend:

Loggers in:

- Stream
- Abandoned channel
- Rest of floodplain
- Outside floodplain

Maximum value
Q3
Average value
Median value
Q1
Minimum value

Morphological features:

- *Top of hillslope (pre-disturbance, 1965)*
- *Base of hillslope (pre-disturbance, 1965)*
- *Abandoned channel*
- *Flow direction*

DEM (m. a.s.l.)

High: 18.6
Mid: 17.0
Low: 14.5

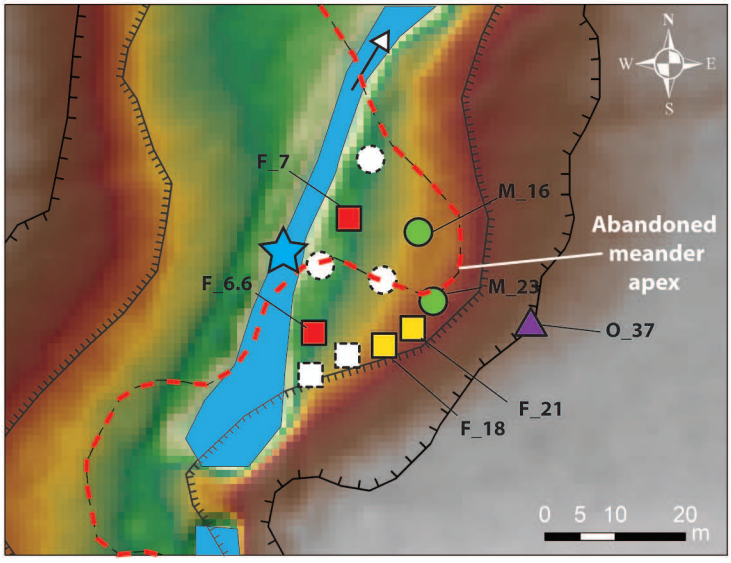

Legend

- *Channel logger*
- *Piezometers in the stream limit of the (historical) floodplain* **(F_6.6, F_7)**
- *Piezometers in the lateral limit of the (historical) floodplain* **(F_18, F_21)**
- *Piezometers in the abandoned meander* **(M_16, M_23)**
- *Piezometers outside the (historical) floodplain* **(O_37)**
- *Elevation (m a.s.l):* High : 18.6 / Low : 15.4
- *Precipitation:*
- *Gradient inversion (during overbank hydrological events:*
- *Head data not displayed:*
- *Fluvial features:*
  - Top of hillslope (pre-disturbance)
  - Base of hillslope (pre-disturbance)
  - Abandoned channel
  - Flow direction
  - Actual stream

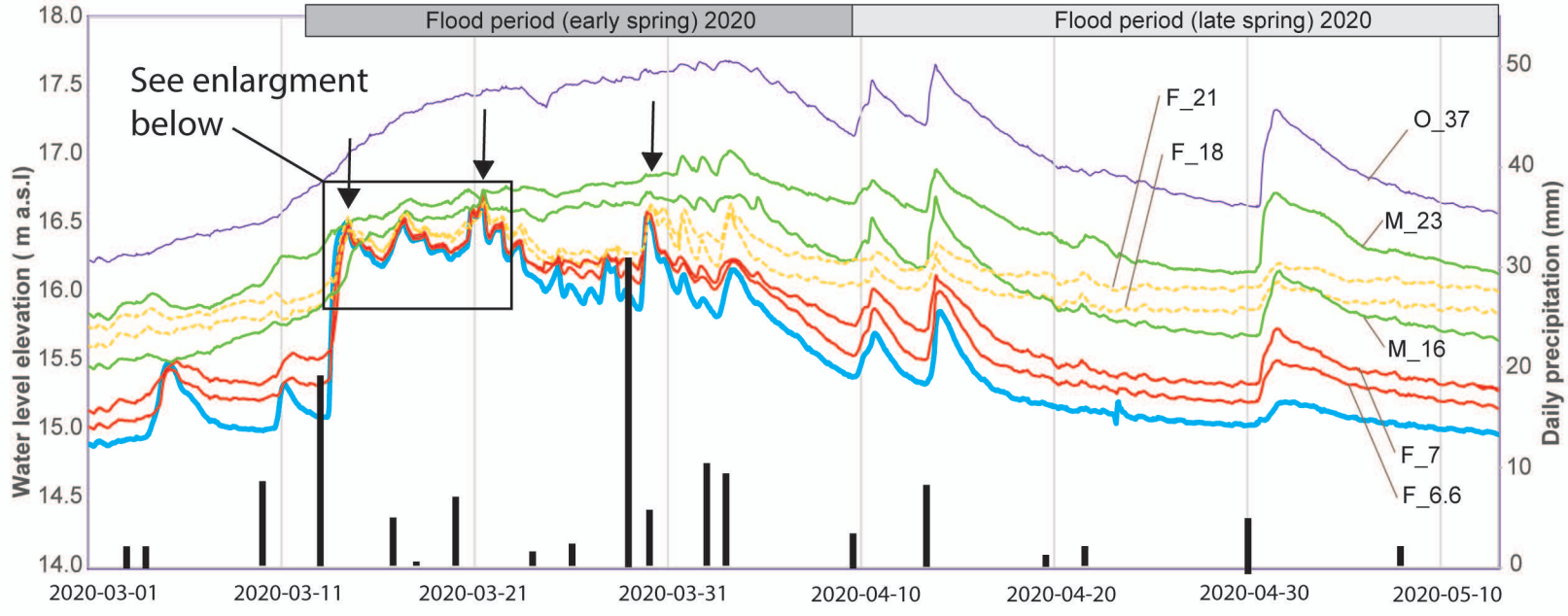

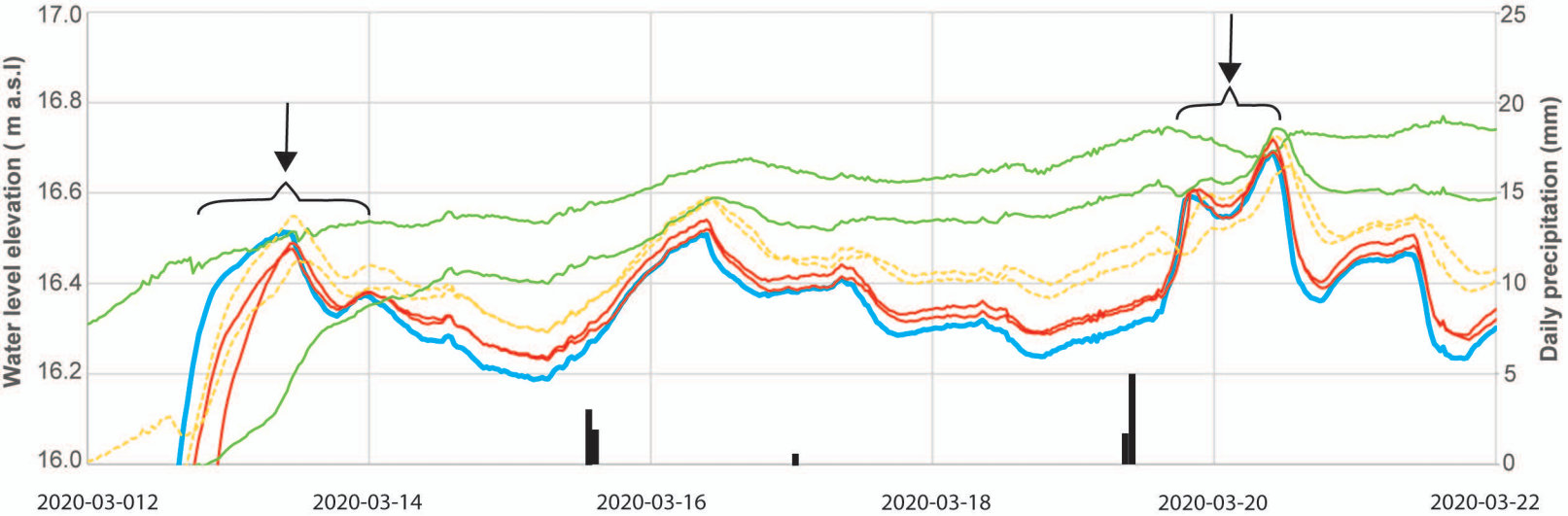

LOW FLOW PERIOD EVENTS

Variables	Petit-Pot-au-Beurre	Martin-UP-Left	Martin-UP-Right	Martin-DS
1 Avg MCCC	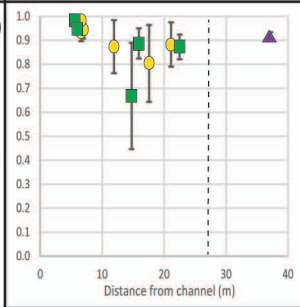	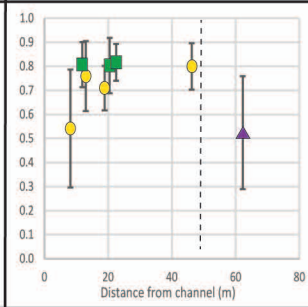	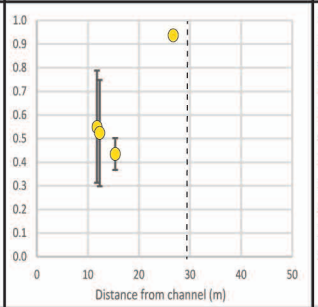	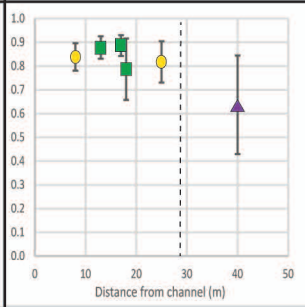
2 Avg Lag	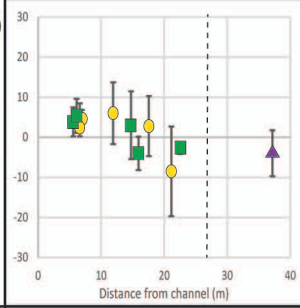	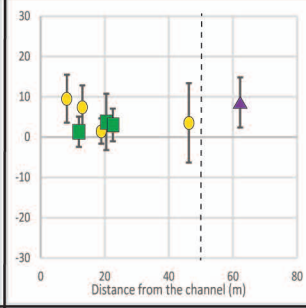	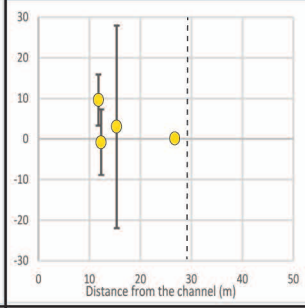	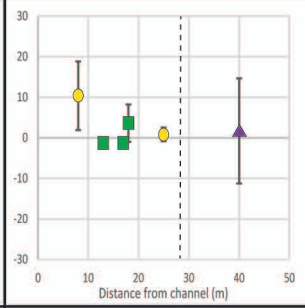
3 Avg amplitude ratio	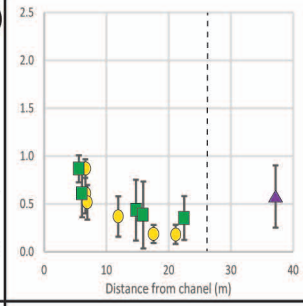	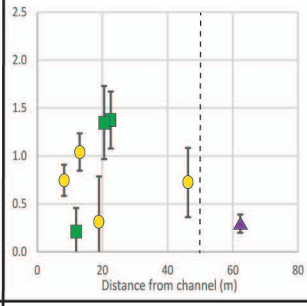	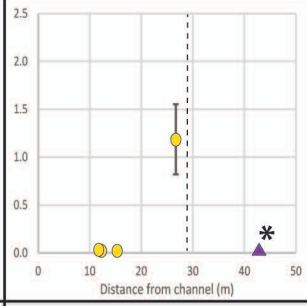	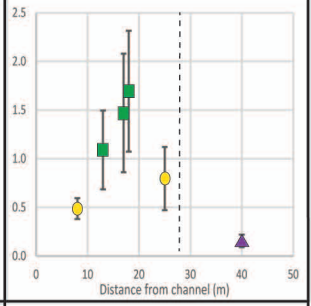
4 Avg duration ratio	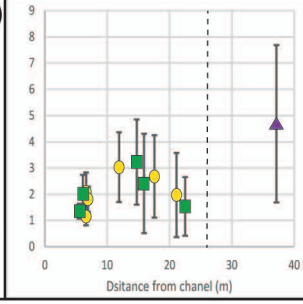	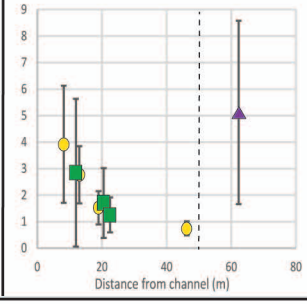	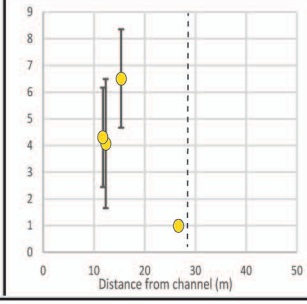	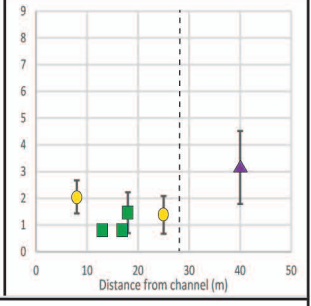

LEGEND:
- Piezometers located within the abandoned meander
- Piezometers in the rest of the floodplain
- Piezometers outside the floodplain
- Standard error (p-value: 0.95)
- * No fluctuation recorded (entire study period)
- Limit of hillslope

Petit-Pot-au-Beurre (PB) - LOW FLOW PERIOD

Hydraulic head (m a.s.l)

Dominant hydraulic gradient

WL M5.6 M6.1 F6.6 F6.9 F7 F12 M14 M16 F18 F21 M23 O37

Distance from channel (m)

Surface elevation

Water table depth (m)

M5.6 M6.1 F6.6 F6.9 F7 F12 M14 M16 F18 F21 M23 O37

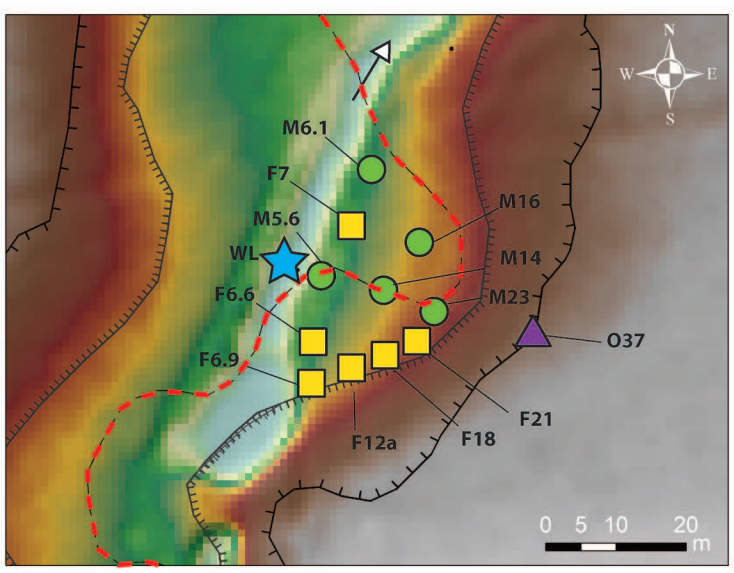

LEGEND:

Loggers in:

- Surface water
- Abandoned channel
- Rest of floodplain
- Outside floodplain

Maximum value
Q3
Average value
Median value
Q1
Minimum value

Morphological features:

- *Top of hillslope (pre-disturbance, 1965)*
- *Base of hillslope (pre-disturbance, 1965)*
- *Abandoned channel*
- *Flow direction*

DEM (m. a.s.l.)

High: 18.6
Mid: 17.0
Low: 14.5

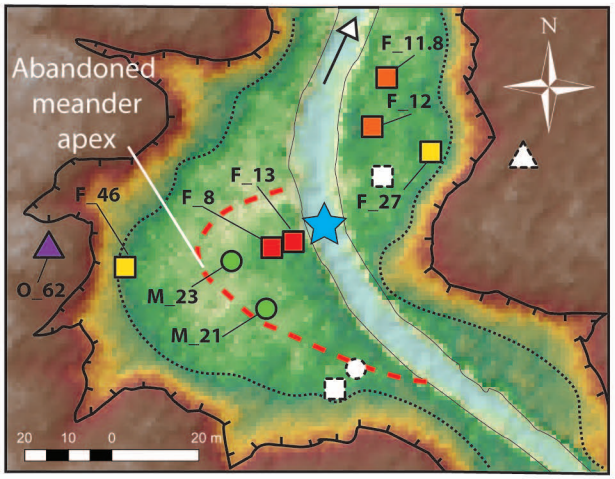

Legend

- *Channel logger*
- *Piezometers in the stream limit of the (left) floodplain (**M_8, M_13**)*
- *Piezometers in the abandoned meander (**M_21, M_23**)*
- *Piezometers outside the floodplain (**O_62**)*
- *Piezometers in the lateral limit of the floodplain (**F_27, F_46**)*
- *Piezometers in the stream limit of the (right) floodplain (**F_11.8, F_12**)*
- *Head data not displayed:*

Precipitation:

Fluvial features:

- Top of hillslope
- Base of hillslope
- Abandoned channel
- Actual channel
- Flow direction

*Water depth (m) (**only for B**)*: 3.0, 1.0, -1.0

A

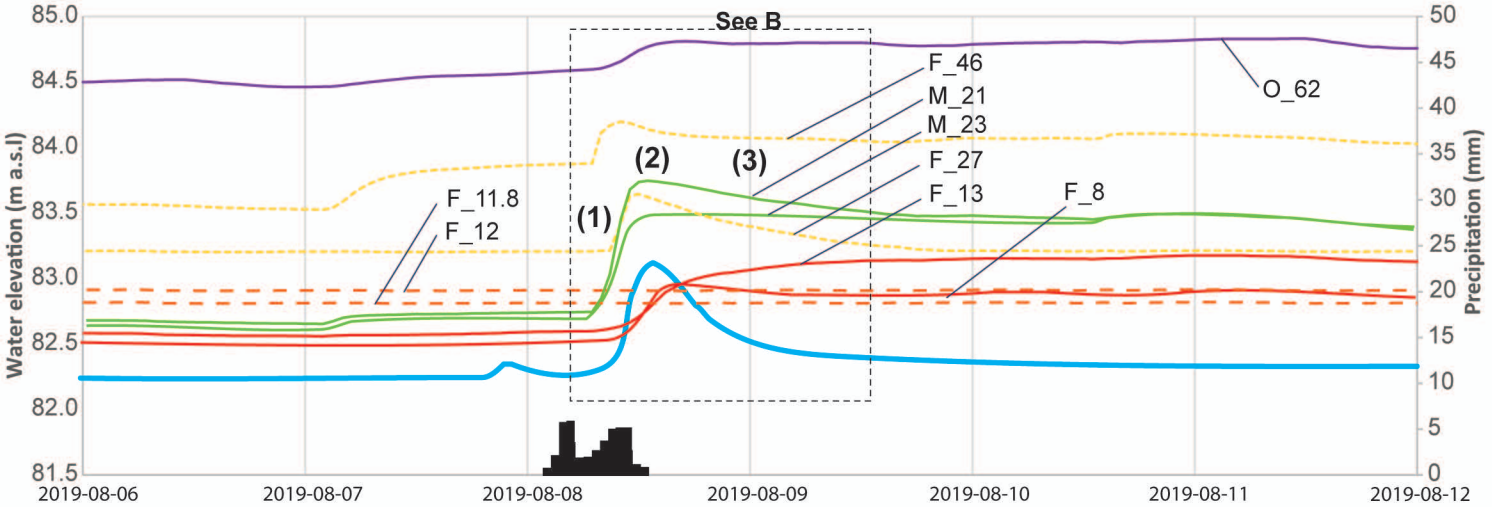

B

(1) 2019-08-08, 7:00 AM, Pre-event

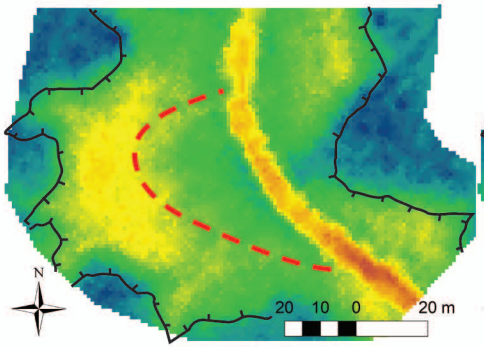

(2) 2019-08-08, 12:00 PM, Peak

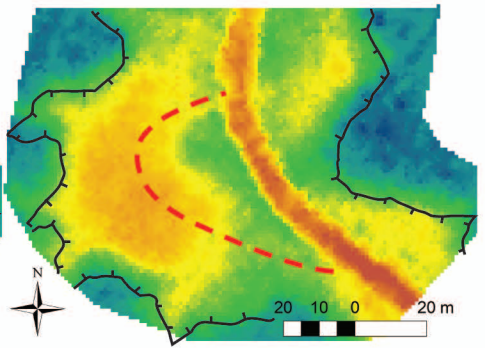

(3) 2019-08-09, 12:00 PM, Post-event

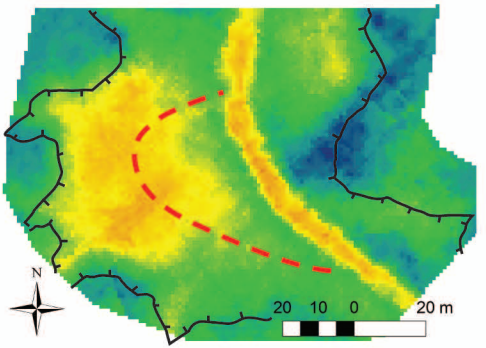

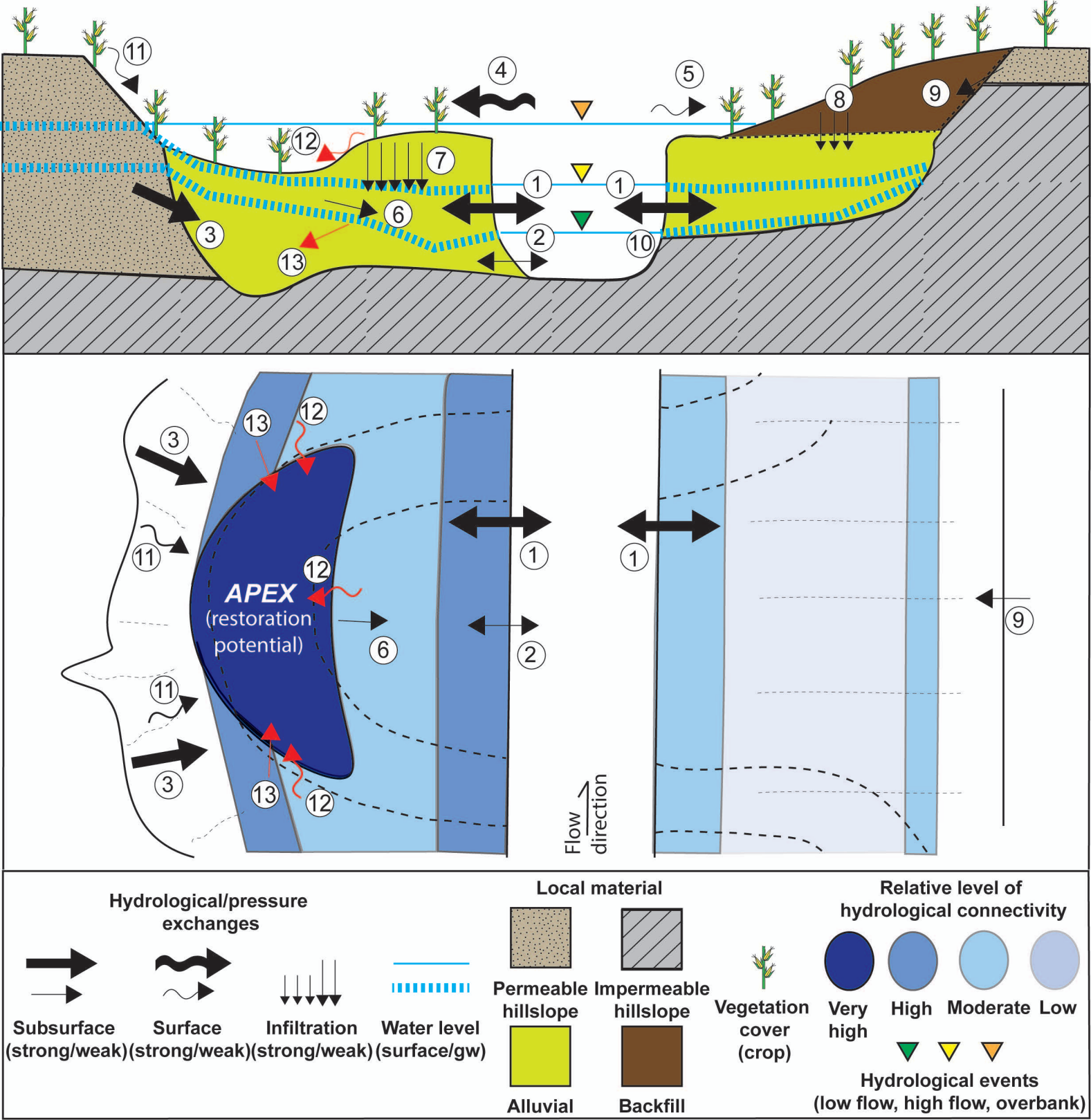
11
4
5
8
9
12
7
1
1
6
3
2
10
13
APEX
(restoration
potential)
Flow
direction
Hydrological/pressure
exchanges
Subsurface
(strong/weak)
Surface
(strong/weak)
Infiltration
(strong/weak)
Water level
(surface/gw)
Local material
Permeable
hillslope
Impermeable
hillslope
Alluvial
Backfill
Vegetation
cover
(crop)
Relative level of
hydrological connectivity
Very
high
High
Moderate
Low
Hydrological events
(low flow, high flow, overbank)

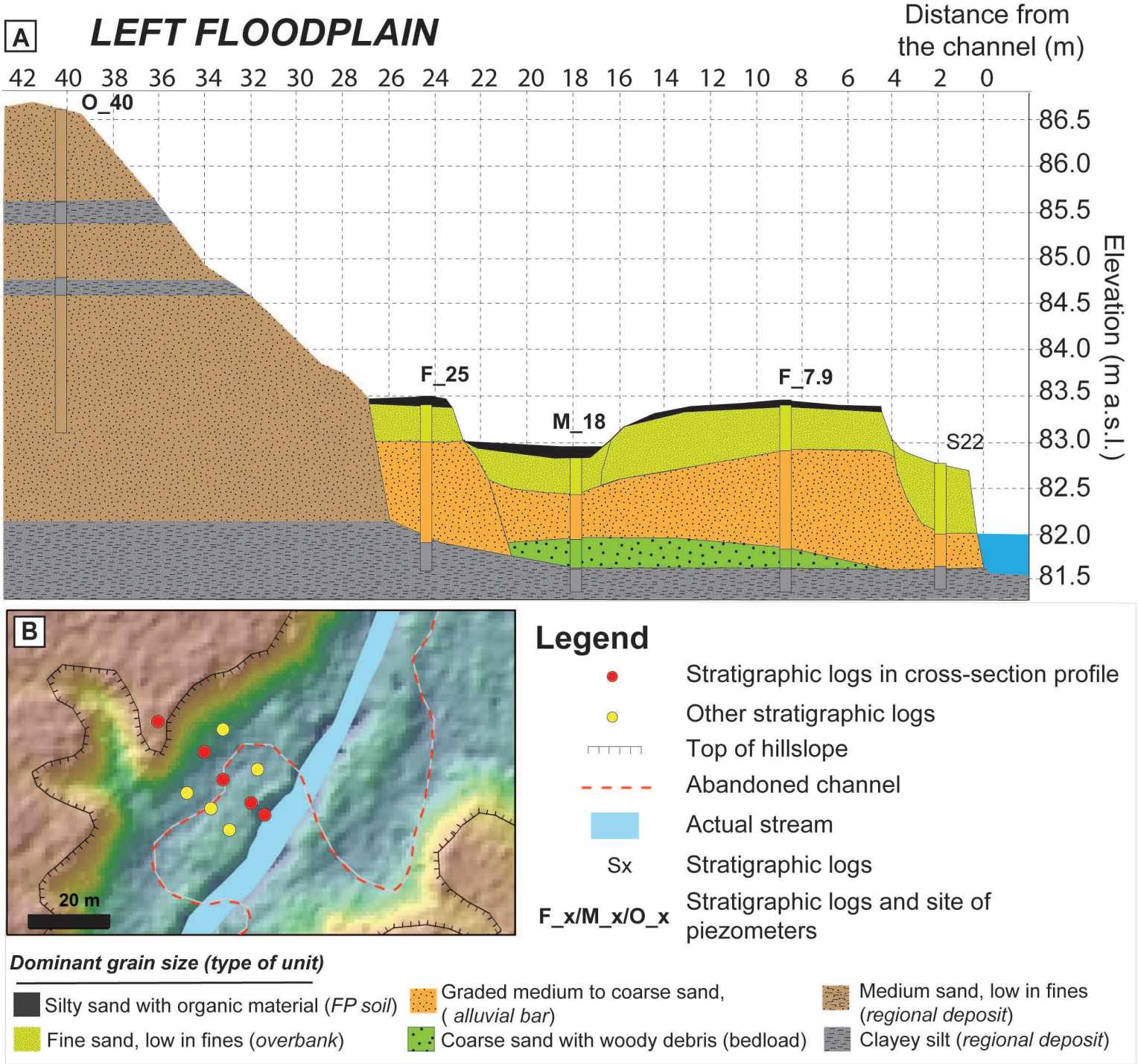

Figure A. (A) Stratigraphic cross-section profile at RM-MID site, representing the left floodplain (looking downstream). Borehole logs labelled with S (ex. S_22) were only used for the stratigraphic characterization. Borehole logs labelled with M (ex. M_18), F, and O were also used for the piezometer installation. Note a vertical exaggeration of 4×. (B) Digital elevation model of the RM site, with the position of the former and actual channel. Red dots indicate the stratigraphic logs that were used to build the cross-section profile.

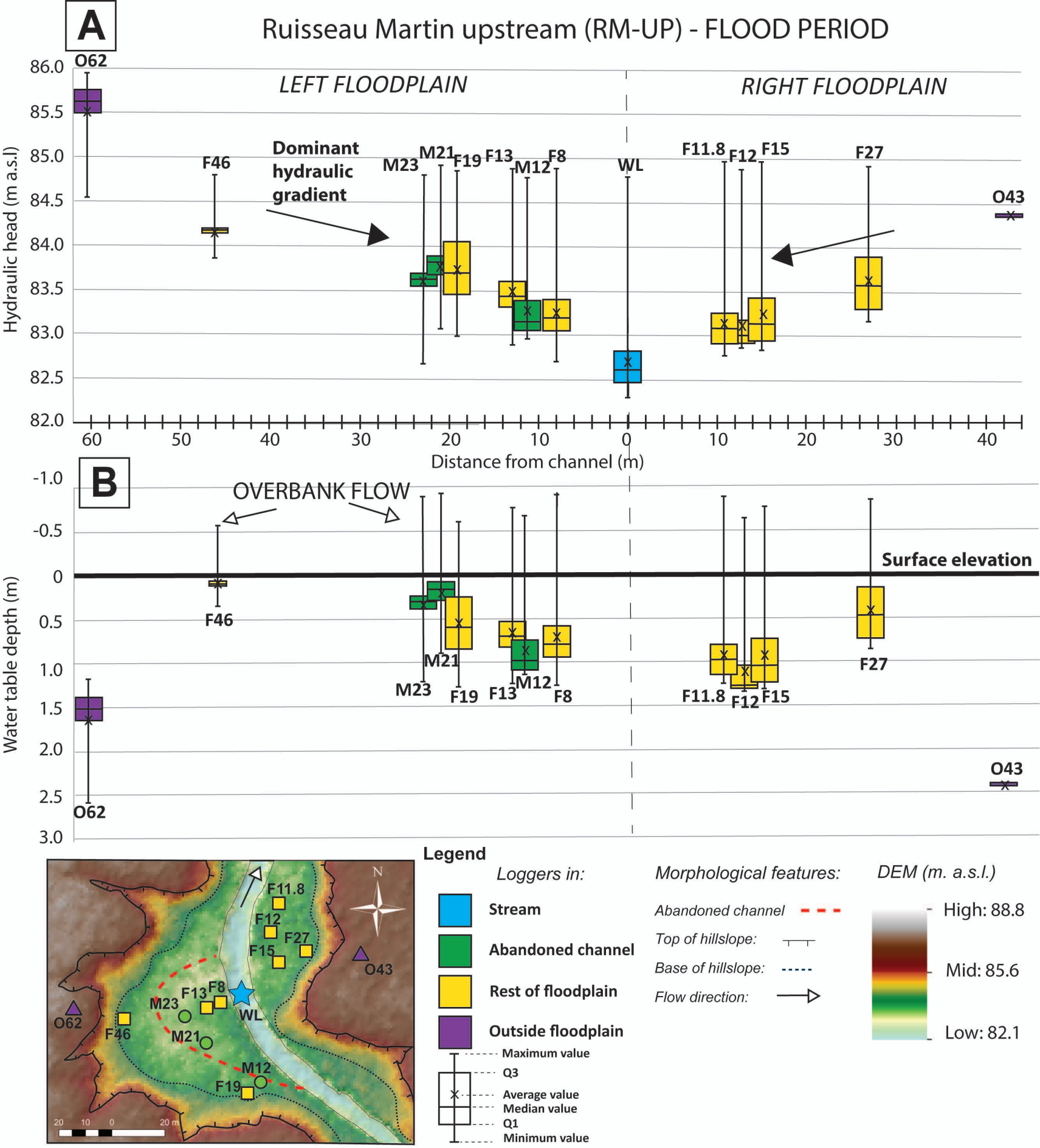

Figure B. Box plot graphs showing A) hydraulic head elevation and B) water depth of piezometers installed at the Ruisseau Martin upstream sites for the flood period (mid-March to mid-May and early October to late December). Negative water depth values indicate water level above the surface.

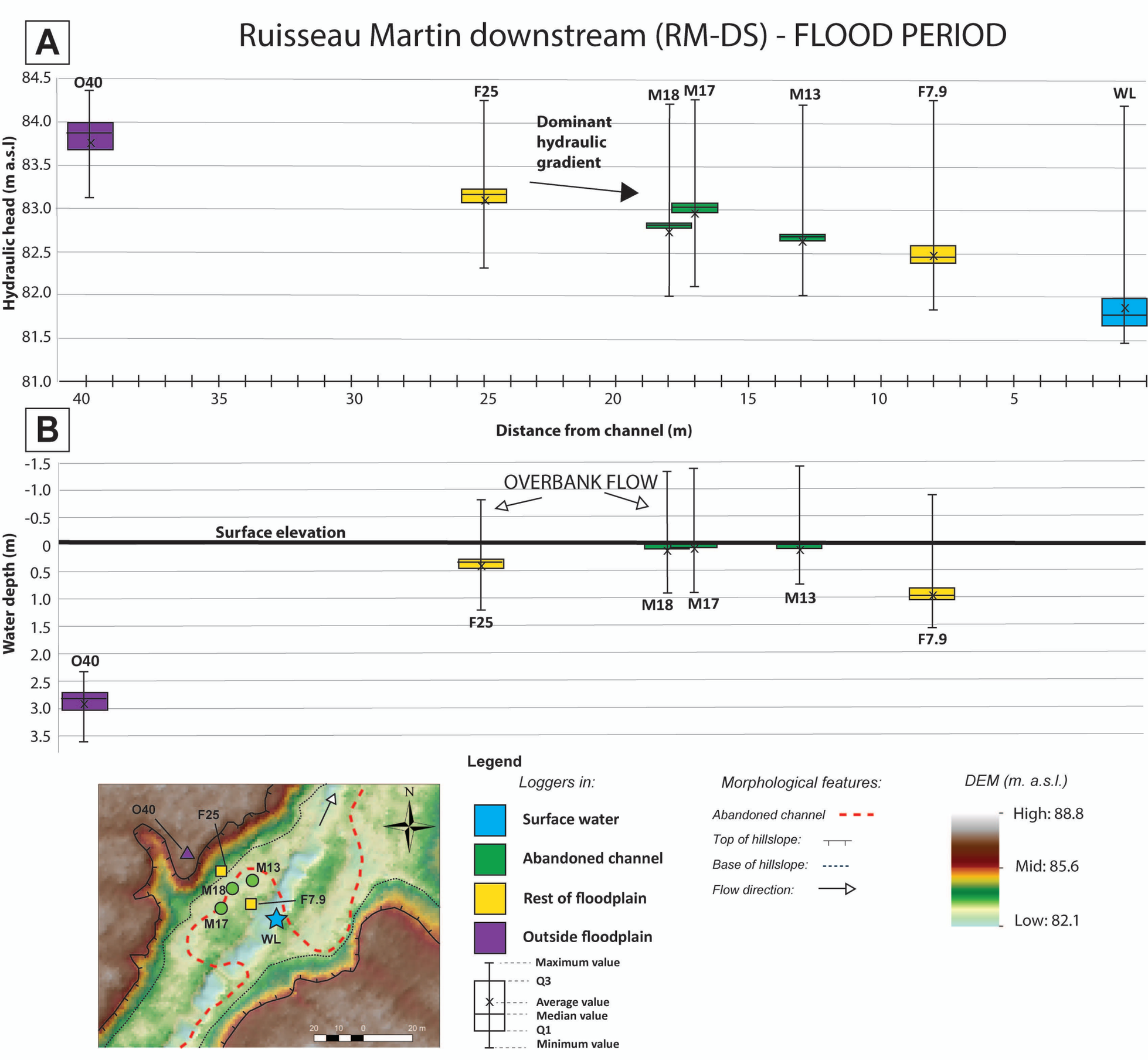

Figure C. Box plot graphs showing A) hydraulic head elevation and B) water depth of piezometers installed at the Ruisseau Martin downstream site for the flood period (mid-March to mid-May and early October to late December). Negative water depth values indicate water level above the surface.

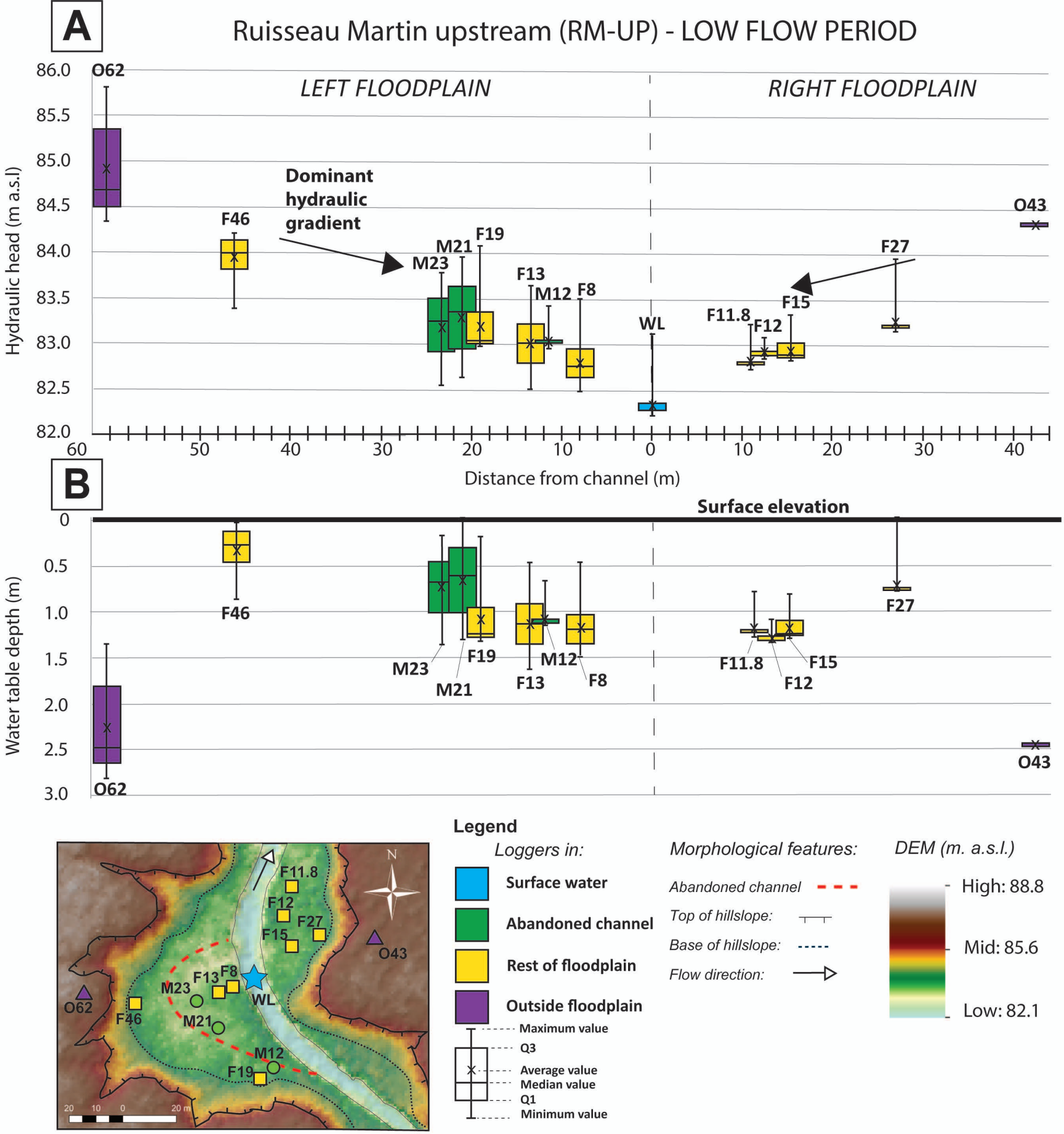

Figure D. Box plot graphs showing A) hydraulic head elevation and B) water depth of piezometers installed at the Ruisseau Martin upstream sites for the low flow period (mid-May to early October).

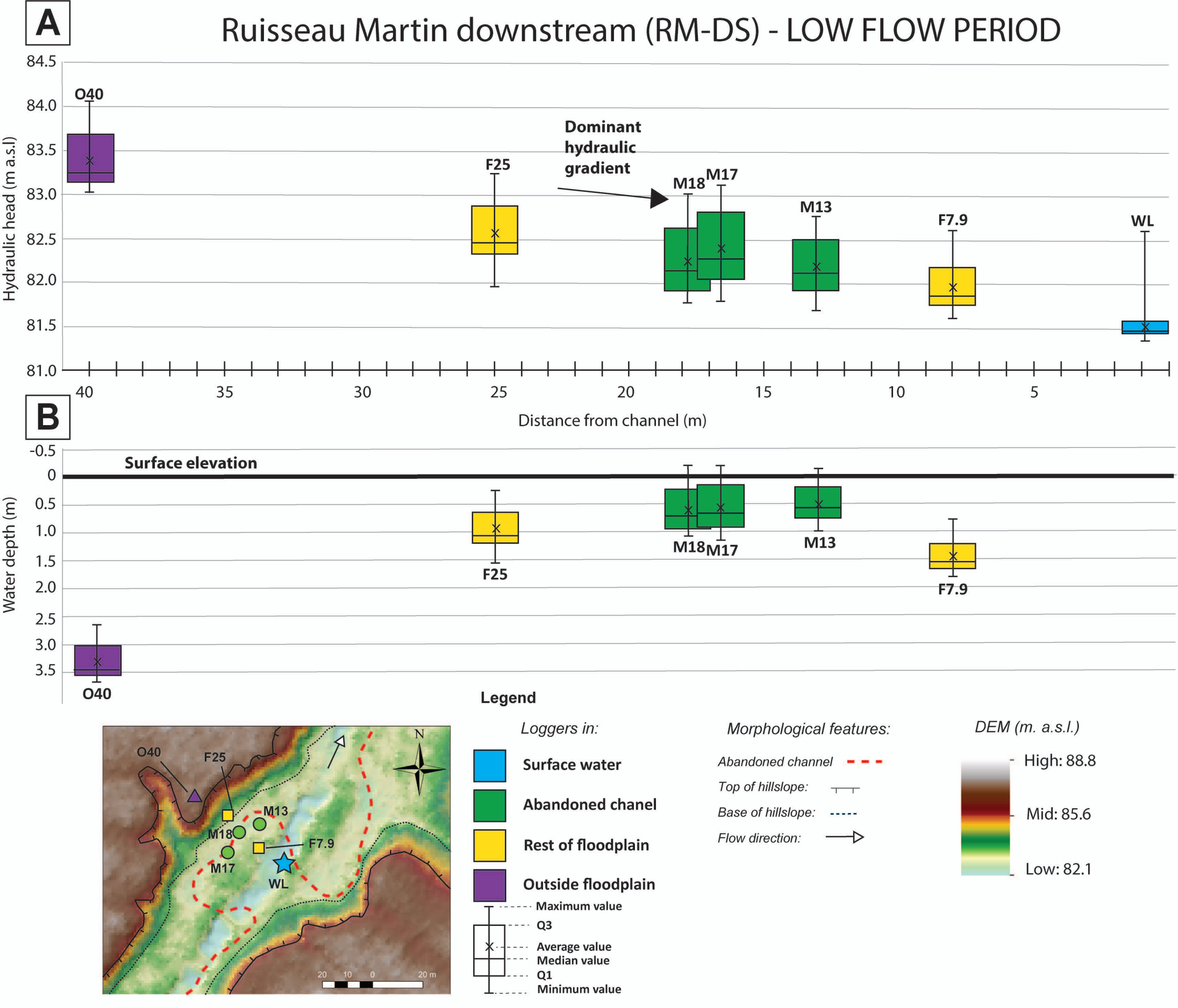

Figure E. Box plot graphs showing A) hydraulic head elevation and B) water depth of piezometers installed at the Ruisseau Martin downstream site for the low flow period (mid-May to early October). Negative water depth values indicate water level above the surface.